# Optimal Hive Management under Uncertainty: should I stay or should I go?

Francesco Campigli* Luca Di Corato†

23 February 2026

**Abstract**

Climate change is increasing environmental variability and reshaping the spatial distribution of floral resources, challenging traditional sedentary beekeeping. Migratory beekeeping (hive mobility) offers a potential adaptation strategy by allowing colonies to track favorable phenological conditions. However, it entails sunk costs and exposure to uncertainty, making hive mobility a dynamic, state-contingent timing decision rather than a static profitability comparison. We develop a continuous-time real-options model in which a beekeeper can switch reversibly between sedentary and migratory management, facing correlated stochastic returns and regime-specific switching costs. The model generates endogenous conversion thresholds and an inaction region. We bring the model to the data using a high-frequency hive-level panel covering 2019–2024, which combines internal weight measurements with geolocation information. Hive-weight dynamics, used as a proxy for productivity, are highly persistent and non-stationary, supporting a stochastic-trend specification. Estimated regime-specific processes show that migratory beekeeping is systematically less volatile and, in most years, characterized by higher expected growth. Observed relocations are predominantly south-to-north and upslope, consistent with climate-driven adaptation. Calibrated policy analysis reveals a sizable option value of migration, infrequent but economically meaningful switching, and rare reversals within an annual horizon. Reducing informational and logistical frictions further increases the adaptive value of mobility.

**Keywords**: Beekeeping; Adaptation to Climate Change; Migration; Climate Variability; Uncertainty; Real Options.

**JEL Classification**: C61, Q54, R11.

*Department of Economics, University of Florence, Via delle Pandette, 50127 Florence, Italy. Email address: francesco.campigli@unifi.it.

†Corresponding author: Department of Economics, Ca' Foscari University of Venice, San Giobbe, Cannaregio 873, 30121 Venice, Italy. Email address: luca.dicorato@unive.it. Telephone: +390412347668.

# 1 Introduction

Climate change is increasing environmental variability and altering the spatial distribution of ecological resources, thereby challenging established agricultural management practices. Beekeeping is particularly exposed to these changes because honeybee productivity depends directly on weather conditions, ecosystem stability, and the spatial and temporal availability of floral resources. Rising temperatures, altered precipitation patterns, and more frequent extreme events affect colony health, foraging behavior, and honey yields, placing pressure on the economic sustainability of apiculture (Neumann and Straub, 2023, Zapata-Hernández et., 2024).

In response to these challenges, beekeepers adopt a range of adaptive strategies, including changes in feeding practices, habitat management, and the relocation of apiaries (Vercelli et al., 2021). Among these, migratory beekeeping, the relocation of hives across space to track favorable flowering conditions, plays a central role as a climate adaptation strategy. Migration can increase expected yields by following phenological gradients and can reduce risk by diversifying exposure across regions. However, it also requires investments in transport and infrastructure, entails regulatory and logistical costs, and exposes beekeepers to additional sources of uncertainty. Moreover, reverting from migratory to sedentary management entails additional sunk costs, making mobility economically reversible in theory but costly and state-dependent in practice.

These features make the choice between sedentary and migratory beekeeping fundamentally different from a static profit comparison. First, both practices are characterized by stochastic returns, reflecting weather variability, ecological dynamics, and market conditions. Second, switching between practices involves sunk costs that cannot be fully recovered. Third, beekeepers can delay switching decisions and learn about future profitability as uncertainty unfolds. Together, these characteristics imply that the decision to adopt or abandon migratory management has an option value that depends on the persistence, volatility, and cross-regime correlation of productivity shocks.

Despite the growing empirical literature on climate impacts and adaptation in beekeeping, existing studies largely focus on realized outcomes or descriptive patterns of mobility, and do not explicitly model the timing and dynamics of reversible switching between management practices under uncertainty. In particular, there is limited formal analysis of how uncertainty, correlation across locations, and sunk switching costs jointly shape optimal mobility decisions over time.

In this paper, we develop a continuous-time real-options model to study a beekeeper's optimal switching decision between sedentary and migratory beekeeping. Each practice generates a stochastic net return process with its own drift and volatility, and shocks to the two processes may be correlated due to common environmental, climatic and market forces. The beekeeper is assumed to be risk-neutral and can switch between practices at any point in time by incurring a practice-specific sunk cost. Framing migration as a costly but reversible investment allows us to characterize the decision problem as an optimal switching problem governed by a system of variational inequalities.

The model yields two endogenous switching thresholds: one governing the transition from sedentary to migratory beekeeping and another governing the reverse transition. The region between

these thresholds defines an inaction region, within which it is optimal to maintain the current practice even if the alternative appears temporarily more profitable. As standard in the real-options models allowing for two-way decisions, uncertainty and sunk costs generate hysteresis: favorable shocks may trigger migration, but equally unfavorable shocks do not necessarily induce an immediate return to sedentary management.

Our contribution is threefold. First, we provide a tractable decision-theoretic framework that formalizes migratory beekeeping as a real-options problem with two-way switching, highlighting how both return enhancement (higher expected growth) and risk mitigation (lower volatility) contribute to the value of mobility. Second, we bring new empirical evidence on climate-driven mobility using a high-frequency hive-level panel (2019-2024) with precise weight measurements and relocation data, documenting strong non-stationarity and persistence in hive-weight dynamics and systematic south-to-north and upslope movements, consistent with following the spring front and cooler, later-blooming environments. Third, we calibrate the model using estimated drift and volatility parameters and quantify the economic value of migration under realistic switching costs.

We find that migration carries systematic option value under climate uncertainty, with short-run relocations occurring far more frequently than shifts to sedentary beekeeping. These findings have important implications for climate adaptation policy: reducing informational frictions and regulatory barriers can further expand the range of conditions under which migration is privately optimal. Beyond beekeeping, the framework applies more broadly to land-based activities in which producers choose between location-bound and mobile strategies under uncertain and spatially correlated productivity.

## 2 Related Literature

### 2.1 Climate change and honey bees

Beekeeping is increasingly recognized as a climate-sensitive agricultural activity, as honey bee colonies depend directly on climatic conditions and indirectly on climate-induced changes in floral resources, phenology, and disease dynamics (Le Conte and Navajas, 2008; Neumann and Straub, 2023; Zapata-Hernández et al., 2024). Recent syntheses show that climate change impacts on apiculture arise from interacting stressors rather than isolated drivers, including rising temperatures, altered precipitation regimes, extreme weather events, forage scarcity, and pathogens (EFSA, 2021; Zapata-Hernández et al., 2024). These pressures threaten both colony viability and the economic sustainability of beekeeping, particularly in regions characterised by high climatic variability such as Mediterranean and semi-arid systems (Flores et al., 2019; Gajardo-Rojas et al., 2022; Van Espen et al., 2023).

Climate change affects honey bees through both direct physiological stress and indirect ecological pathways (Le Conte and Navajas, 2008; Ostwald et al., 2024). As ectothermic organisms, honey bees are highly sensitive to temperature variation, which regulates brood development, foraging activity, and colony thermoregulation (Le Conte and Navajas, 2008). Increasing temperatures and

more frequent heat extremes raise energetic costs for cooling, disrupt brood regulation, and reduce foraging efficiency, ultimately constraining colony growth and survival, especially in regions where heatwaves and droughts co.occur (Flores et al., 2019; Neumann and Straub, 2023; Ostwald et al., 2024). At the same time, altered precipitation regimes and drought reduce floral abundance, nectar secretion, and pollen quality, intensifying nutritional stress during critical phases of colony development (Gajardo-Rojas et al., 2022; Zapata-Hernández et al., 2024).

These climatic pressures increasingly operate through spatio-temporal mismatches between colony demand and floral availability, reinforcing the spatial dimension of climate vulnerabilit (Van Espen et al., 2023; Mahankuda and Tiwari, 2024). Empirical work in Mediterranean environments documents erratic flowering, loss of monofloral honeys, and shortened or irregular nectar flows, increasing the risk of resource gaps for colonies (Flores et al., 2019; Vercelli et al., 2021). As a result, beekeeping becomes less viable in fixed locations, particularly where droughts and extreme events recur frequently (Neumann and Straub, 2023).

Modelling studies reinforce this spatial dimension of vulnerability. Species distribution models identify temperature seasonality, precipitation, and solar radiation as key predictors of honey bee habitat suitability, projecting strong contractions or shifts of highly suitable areas for Apis mellifera under future climate scenarios (Tennakoon et al., 2024). At the global scale, similar modelling indicates widespread losses of climatically suitable habitat for bees, with strong regional contrasts (Huang et al., 2022; Rahimi and Jung, 2024). Together, these findings suggest that climate change is reshaping the geography of viable beekeeping and pollination services, not merely intensifying existing stressors (Zapata-Hernández et al., 2024; Neumann and Straub, 2023).

In response to growing climatic variability, beekeepers increasingly adopt management strategies aimed at buffering colonies against stress, including supplementary feeding, intensified disease control, selective breeding, and habitat restoration (Le Conte and Navajas, 2008; Neumann and Straub, 2023). Survey and qualitative studies show that such strategies are now widely adopted across Europe, the Americas, and Asia as beekeepers respond to more unpredictable seasons and declining yields (Gajardo-Rojas et al., 2022; Vercelli et al., 2021; Van Espen et al., 2023). However, these measures largely operate at the local scale and do not address the broader spatial redistribution of floral resources and climatic suitability induced by climate change (EFSA, 2021).

Empirical evidence illustrates these limits. In drought-prone regions of Chile, forage shortages often persist beyond the capacity of feeding or management interventions, leading to declining honey yields and increased colony losses (Gajardo-Rojas et al., 2022). Similar patterns, reduced nectar availability, loss of traditional honey types, and compromised overwinter survival, are described by Mediterranean beekeepers in Italy and Spain (Flores et al., 2019; Vercelli et al., 2021). Nutritional stress also interacts with disease dynamics, as weakened colonies become more susceptible to pathogens and parasites, while warmer conditions may favour pests such as Varroa destructor, Nosema spp. (EFSA, 2021; Mahankuda and Tiwari, 2024).

Against this background, migratory beekeeping (transhumance) emerges as a key spatial adaptation strategy. By relocating colonies seasonally, beekeepers can track favourable flowering conditions

and climatic regimes, reducing exposure to prolonged forage shortages and phenological mismatches (Swapna et al., 2023; Neumann and Straub, 2023). Mobility directly addresses the spatio-temporal reorganisation of resources that characterises climate-change impacts on agro-ecosystems and underpins both honey production and crop-pollination contracts in many regions (Martinez-Lopez et al., 2022).

Empirical studies provide strong support for this role. In Chile, prolonged megadrought conditions in Mediterranean regions were associated with sharp declines in honey production, prompting widespread adoption of transhumance toward regions with more reliable precipitation and floral resources (Gajardo-Rojas et al., 2022). Across Europe, beekeepers, especially in southern regions, report stronger climate impacts and increasingly rely on seasonal movements, including to higher elevations and cooler areas, to stabilise honey yields and reduce winter losses (Van Espen et al., 2023; Neumann and Straub, 2023). Qualitative work in Mediterranean contexts similarly indicates that transhumance has become essential under erratic flowering and recurrent droughts (Vercelli et al., 2021; Remotti et al., 2024).

Qualitative evidence further highlights how climate change is experienced as a loss of predictability that incentivises mobility. Beekeepers describe increasingly frequent droughts, late frosts, and unstable seasons that disrupt traditional honey flows and force reactive responses such as emergency feeding or relocation (Remotti et al., 2024). Similar perceptions of greater climatic irregularity and more frequent "bad years" are reported across Europe, linking climate change to lower yields and increased management effort (Van Espen et al., 2023).

Conceptually, migratory beekeeping restores synchrony between colonies and floral resources when local conditions deteriorate, and is widely framed as a climate-adaptation strategy in the literature (Neumann and Straub, 2023; Zapata-Hernández et al., 2024). This aligns with broader frameworks describing migration as an "escape strategy" under climate stress, allowing production systems to temporarily decouple from unfavourable local condition (Mahankuda and Tiwari, 2024). Economic modelling further suggests that optimising the sequencing of colony movements can significantly influence profitability under environmental variability (Pilati and Fontana, 2020).

Despite its adaptive value, migratory beekeeping involves important trade-offs. Reviews indicate a tendency toward higher prevalence of pathogens and parasites in mobile colonies, linked to transport stress, aggregation of colonies at pollination sites, pesticide exposure, and contact with novel pathogen pools (Martinez-Lopez et al., 2022; EFSA, 2021). Mobility may therefore amplify epidemiological risks if not accompanied by adequate biosecurity and coordinated health monitoring, with potential consequences for both managed and wild pollinators (Zapata-Hernández et al., 2024).

Large-scale colony movements may intensify competition for floral resources and complicate disease governance in landscapes lacking coordinated regulation. Stakeholder studies highlight the need for integrated policy frameworks that jointly address climate stressors, land-use change, pesticide exposure, and disease dynamics, and that consider carrying capacity when concentrating hives in specific areas (EFSA, 2021; Van Espen et al., 2023).

In summary, the literature portrays climate change as a driver of both intensified stress and spatial reconfiguration within beekeeping systems. While local management strategies can mitigate short-term impacts, they do not address the underlying redistribution of climatic suitability and floral resources. Migratory beekeeping therefore emerges as a central adaptation pathway, enabling beekeepers to sustain production by tracking shifting resource landscapes, while simultaneously introducing new disease and governance challenges that must be addressed to ensure long-term sustainability.

### 2.2 Real options and climate adaptation

The analytical foundation of this paper lies in real-options theory, which formalizes decision-making under uncertainty when actions are costly to reverse and can be optimally delayed.[1] A central insight of this framework is that waiting has value because it allows agents to acquire information about future payoffs as uncertainty unfolds. By postponing action, agents observe new realizations of stochastic returns, update beliefs about future profitability, and preserve the flexibility to act under more favorable conditions. In the presence of uncertainty and sunk costs, investment and disinvestment decisions are therefore governed by trigger thresholds rather than static net present value comparisons. Exercising an option not only incurs partially or fully irreversible costs but also eliminates the option to learn from future information, implying that optimal switching requires a sufficiently large and persistent advantage of the alternative regime to compensate for the forgone informational and flexibility value.

Building on these insights, Schatzki (2003) applies the real-options framework to land-use conversion decisions,[2] allowing for costly reversibility between agricultural and forest uses. He shows that greater return uncertainty raises conversion thresholds, whereas higher correlation between returns lowers them by reducing uncertainty in relative profitability. In a similar framework, Song et al. (2011) develop a two-way real-options model in which farmers can switch between traditional crops and perennial energy crops, incurring sunk costs in both directions. Allowing for reversible but costly switching generates two distinct conversion boundaries, one for adoption and one for reversion, creating an inaction band in which farmers optimally remain in the current land use.

Real-options approaches have also been applied explicitly to climate-change adaptation decisions. Narita and Quaas (2014) conceptualize adaptation as a timing problem under climate variability, demonstrating that agents may optimally delay adaptation even when expected net benefits turn positive. Their analysis shows how uncertainty and learning generate a wedge between static break-even conditions and dynamically optimal switching thresholds, reinforcing the relevance of real-options logic for climate-sensitive production systems. Closely related to the mobility dimension of our model, Di Corato and Ginbo (2021) analyze relocation decisions of coffee farms under climate change using a real-options framework. They show that optimal relocation

[1] See Dixit and Pindyck (1994) for an exhaustive treatment of real-options theory.

[2] See Regan et al. (2015) for a comprehensive review of real-options applications to land-use management.

requires returns at the new location to exceed not only operating costs but also an additional option-value component induced by uncertainty.

Taken together, this literature motivates our modeling strategy in three key dimensions: (i) uncertainty makes the timing of switching central; (ii) sunk and asymmetric switching costs generate inaction regions and hysteresis; and (iii) correlation in stochastic returns critically shapes optimal switching by influencing uncertainty in relative profitability. Our contribution extends these insights to migratory beekeeping as a climate-adaptation strategy, a context in which costly mobility and correlated environmental shocks play a defining role.

# 3 The model

The decision to switch from sedentary to migratory beekeeping can be interpreted as a partially irreversible investment under uncertainty. Because switching entails sunk costs, the beekeeper retains the option to wait and observe the evolution of relative profitability over time. This option has value: delaying the switch allows the beekeeper to acquire additional information about future returns before committing to a costly and only partially reversible change in management practice. Higher uncertainty in the profitability of either practice increases the value of waiting and therefore delays switching, whereas stronger correlation between sedentary and migratory returns reduces uncertainty in relative performance, thereby making switching more likely. These forces generate an inaction region, and imply hysteresis in management choices: a favorable shock may induce adoption of migratory beekeeping, but an equally unfavorable shock is typically insufficient to trigger an immediate return to sedentary management.

We formalize this intuition in a continuous-time setting as follows.[3] We consider a risk-neutral beekeeper[4] who manages a single hive and faces a dynamic decision between two alternative management regimes: sedentary beekeeping, denoted by $s$, and migratory beekeeping, denoted by $m$. At any point in time, the beekeeper may either continue operating under the current regime or switch to the alternative regime. Switching from regime $i$ to regime $j$, with $i, j \in \{s, m\}$ and $i \neq j$ entails a sunk cost $K_{ij}$, which cannot be recovered once incurred.

Let $\pi_i(t)$, with $i \in \{s, m\}$, denote the instantaneous net return associated with regime $i$. Net returns are assumed to follow a geometric Brownian motion (GBM):

$$d\pi_i(t) = \mu_i \, \pi_i(t) \, dt + \sigma_i \, \pi_i(t) \, dz_i(t), \qquad i \in \{s, m\}. \tag{1}$$

where $\mu_i$ is the drift (expected growth rate), $\sigma_i$ is the volatility parameter, and $z_i(t)$ is a standard Wiener process. The two Wiener processes are allowed to be correlated:

$$\mathbb{E}[dz_s(t) \, dz_m(t)] = \rho \, dt, \qquad \rho \in [-1, 1]. \tag{2}$$

[3] Our model is closely related to real-options land-conversion frameworks with two-way switching, such as Schatzki (2003) and Song et al. (2011).

[4] For simplicity, we assume risk neutrality; allowing for risk aversion would not alter the qualitative structure of the problem, but would mainly shift the switching thresholds (see Narita and Quaas, 2014).

Let $V_i(\pi_s(t), \pi_m(t))$ denote the value function associated with managing the hive under regime $i \in \{s, m\}$ at time $t$, conditional on the current net returns under both practices. The value function represents the expected discounted payoff obtained when the beekeeper follows an optimal switching strategy from that point onward. Let $r$ denote the constant discount rate.
The beekeeper's dynamic optimization problem satisfies the Bellman equation:

$$V_i(\pi_s(t), \pi_m(t)) = \max\left\{\pi_i(t)\,dt + e^{-r\,dt}\,\mathbb{E}[V_i(\pi_s(t+dt), \pi_m(t+dt))]\,,\; V_j(\pi_s(t), \pi_m(t)) - K_{ij}\right\}, \quad i \neq j. \tag{3}$$

The first term corresponds to continuation under the current regime, while the second captures the option to switch to the alternative regime, net of the corresponding sunk cost.

Applying Itô's Lemma to the value function yields the infinitesimal generator associated with the value function:

$$\Gamma V_i = \; rV_i - \pi_i(t) - \sum_{k=s,m} \mu_k \pi_k(t) \frac{\partial V_i}{\partial \pi_k} - \frac{1}{2} \sum_{k=s,m} \sigma_k^2 \pi_k^2(t) \frac{\partial^2 V_i}{\partial \pi_k^2} - \rho \sigma_s \sigma_m \pi_s(t) \pi_m(t) \frac{\partial^2 V_i}{\partial \pi_s \partial \pi_m} \tag{3.1}$$

The two regime-specific value functions must satisfy the following *complementarity conditions*:

$$\Gamma V_i \geq 0, \qquad i \in \{s, m\}, \tag{4}$$

$$V_i(\pi_s, \pi_m) \geq V_j(\pi_s, \pi_m) - K_{ij}, \qquad i \neq j. \tag{5}$$

At each point in the state space, at least one of these conditions must bind. If the first condition holds with equality, it is optimal to remain in the current regime. If the second condition binds, the beekeeper optimally switches regimes. When both conditions bind, the beekeeper is indifferent between switching and waiting.

The solution is characterized by two endogenous *switching boundaries* in the state space $(\pi_s, \pi_m)$:

- $\pi_m = b_{sm}(\pi_s)$: the threshold for switching from sedentary to migratory beekeeping. When the expected profitability under migratory management is sufficiently high relative to sedentary management, i.e. when $\pi_m > b_{sm}(\pi_s)$, the beekeeper optimally switches from sedentary to migratory beekeeping.

- $\pi_m = b_{ms}(\pi_s)$: the threshold for switching from migratory to sedentary beekeeping. When the expected profitability under migratory management is sufficiently low relative to sedentary management, i.e. when $\pi_m < b_{ms}(\pi_s)$, the beekeeper optimally switches from migratory to sedentary beekeeping.

The region between these two boundaries defines an inaction region, within which it is optimal to maintain the current management regime. As in standard real-options models with sunk costs, the two thresholds generally do not coincide, giving rise to hysteresis in management decisions.

Because the value functions $V_s$ and $V_m$ are mutually interdependent, closed-form solutions are not available. We therefore approximate them numerically using a collocation method, expressing each value function as:

$$\hat{V}_i(\pi_s, \pi_m) = \sum_{j_s=1}^{n_s} \sum_{j_m=1}^{n_m} q_{j_s j_m} \, \phi_{j_s j_m}(\pi_s, \pi_m) \tag{6}$$

where $\phi_{j_s j_m}$ are basis functions (e.g., piecewise linear splines), and the coefficients $q_{j_s j_m}$ are chosen so that the optimality conditions are satisfied at a predefined set of interpolation nodes.

### 3.1 Net returns, normalization, and choice of exogenus parameters

The empirical implementation focuses on a representative beekeeper's optimal hive management problem under uncertainty. We consider a beekeeper operating a single hive that can be managed either under a sedentary regime or under migratory management. We assume that the hive is initially managed under the sedentary regime, while migratory beekeeping represents the alternative regime. To calibrate the stochastic switching model using observable economic magnitudes, we express instantaneous net returns per hive as proportional to hive productivity. Specifically, net returns under regime $i \in \{s, m\}$ are defined as

$$\pi_i(t) \;=\; \pi_{i,2024} \, a_i(t), \tag{7}$$

where $\pi_{i,2024} > 0$ denotes baseline net revenue per hive under regime $i$ in 2024, and

$$a_i(t) \;=\; \frac{w_i(t)}{\overline{w}_{i,2024}} \tag{7.1}$$

is a dimensionless hive-unit variable obtained by normalizing the hive weight $w_i(t)$ by the average hive weight $\overline{w}_{i,2024}$ observed under regime $i$ in 2024. This normalization anchors the model to observed sectoral benchmarks and ensures that $a_i(t) = 1$ corresponds to a representative hive in 2024.

Hive weight is assumed to evolve according to a geometric Brownian motion (GBM),

$$dw_i(t) \;=\; \mu_i \, w_i(t) \, dt + \sigma_i \, w_i(t) \, dz_i(t), \qquad i \in \{s, m\}, \tag{8}$$

where $\mu_i$ and $\sigma_i$ denote drift and volatility parameters, and $z_i(t)$ is a standard Wiener process. Under this specification, net returns inherit the same stochastic dynamics as in the switching model, ensuring internal consistency between empirical estimation and the theoretical framework.

Due to data limitations, fluctuations in hive weight, and therefore in yields, are treated as the sole source of uncertainty. This assumption is not restrictive for the switching decision for two main reasons. Under the maintained hypothesis that output quality is comparable across regimes, price shocks would affect sedentary and migratory returns symmetrically, while operating costs, although differing in levels, are plausibly highly correlated over time. If time-varying prices $p_i(t)$

and costs $c_i(t)$ were available, net returns could instead be written as $\pi_i(t) = (p_i(t) - c_i(t))w_i(t)$, and an arithmetic Brownian motion would naturally accomodate the possibility of negative profits. In the present context, however, the multiplicative GBM specification provides a parsimonious and empirically grounded representation.

Let $\{w_t = (w_{s,t}, w_{m,t})\}_{t=0,\dots,N}$ denote observed hive weights sampled every $\Delta t = 1/8$ day. Allowing for correlation across regimes, we assume

$$\mathrm{E}[dz_s(t)\, dz_m(t)] = \rho\, dt.$$

By Itô's lemma, log-increments

$$y_{i,t} = \ln\left(\frac{w_{i,t}}{w_{i,t-1}}\right)$$

are jointly Gaussian with mean $(\mu_i - \frac{1}{2}\sigma_i^2)\Delta t$ and covariance matrix $\Sigma\Delta t$, where

$$\Sigma = \begin{pmatrix} \sigma_s^2 & \rho\,\sigma_s\sigma_m \\ \rho\,\sigma_s\sigma_m & \sigma_m^2 \end{pmatrix}.$$

Maximum likelihood estimates of $(\mu_s, \sigma_s, \mu_m, \sigma_m, \rho)$ are obtained by combining a broad random grid search over plausible parameter ranges with local quasi-Newton optimization of the full log-likelihood function. Initial conditions are fixed at the first observed weights, thereby directly anchoring the continuous-time representation to the data. Baseline revenues and costs are taken from the CREA survey (2025, Table 2, "Average Economic Results"). Per-hive revenues are computed as

$$p_i = \frac{\text{Honey + other products}_i}{\#\text{hives}_i},$$

yielding $p_s = 140.95$ and $p_m = 173.02$, while variable costs are $c_s = 56.00$ and $c_m = 65.38$. These differences reflect both scale effects and structural cost heterogeneity across management regimes. Baseline net revenues $\pi_{i,2024} = p_i - c_i$ are used to scale stochastic productivity into monetary units.

We define sunk switching costs $K_{ij}$ as the present value of the stream of periodic fixed costs incurred when switching from practice i to practice j, net of public support, so as to capture only the beekeeper's private net outlay. These costs include hired labor, depreciation, and other fixed costs. The present value is computed using an annual discount rate of 8%. Using the "Fixed Cost" and "Public Support" entries in Table 2 of the CREA survey (2025), we obtain

$$K_{sm} = 866, \qquad K_{ms} = 809.79.$$

Throughout the paper, the annual discount rate is fixed at $r = 0.08$. The empirical and numerical analysis is conducted over a finite horizon corresponding to a single production year ($T = 1$). This choice reflects the operational decision cycle in beekeeping and ensures that all expected discounted payoffs, and the associated value functions, are finite by construction.

Under a finite horizon, the model remains well-defined even if empirically estimated productivity

drifts exceed the annual discount rate in some years (i.e., $\mu_i \geq r$ for some $i$ and years), because the discounted integral is evaluated over $[0, T]$ rather than over $[0, \infty)$. Accordingly, we do not impose the perpetual-payoff convergence condition $r > \mu_i$ required in infinite-horizon formulations with geometric growth.

Although the model is solved over a finite annual horizon ($T = 1$), the diffusion structure implies that, over sufficiently long horizons, boundary crossings occur with probability one under non-degenerate volatility. The finite-horizon formulation therefore reflects the operational decision cycle of beekeeping, without altering the qualitative properties of the switching problem.

# 4 Dataset analysis, geolocalization, mapping hives' movements

This section describes the data infrastructure that links the theoretical switching model to observed adaptive behavior. The empirical analysis relies on a hive-level panel spanning the period 2019-2024. For each monitored hive, we observe internal weight dynamics and spatial coordinates over time. The raw data were provided by 3BEE and processed through a standardized cleaning, alignment, and harmonization workflow designed to ensure temporal consistency and spatial coherence across hive trajectories.. The core variables used in the analysis are hive weight (measured in kilograms) and geolocation (latitude, longitude, and altitude). Each hive is identified by a unique and time-invariant ID, and observations are stored as time series indexed by this identifier. Multiple hive IDs may correspond to the same beekeeper; however, due to European privacy regulations, no personal identifiers are available and hive IDs cannot be linked to individual operators. The empirical unit of analysis is therefore the hive, tracked over time through its internal measurements and spatial location. For every monitored hive, the internal weight variable is available. Weight is measured in kilograms through pressure sensors placed beneath the hive, which report readings from multiple load points. These readings are consolidated into a single weight observation per hive and timestamp, which constitutes the main productivity proxy used in the analysis. In addition to weight, the dataset includes the hive's geographical location over time. Geolocation is recorded as latitude and longitude and complemented by altitude, allowing us to characterize movements both along the latitudinal gradient and along the elevational dimension. A key feature of the raw dataset is that observations are irregularly spaced in time. This irregularity arises because sensor transmissions are not synchronized across hives and because connectivity conditions generate uneven reporting intervals. Because our empirical strategy requires time-consistent trajectories, both to compare hives on a common grid and to align productivity dynamics with relocation episodes, we construct an equally spaced panel by regularizing the time axis. We adopt a three-hour aggregation interval (eight observations per day) and construct, for each hive, a complete three-hour grid spanning the calendar year. Each raw weight reading is assigned to its corresponding three-hour window, and the grid value is defined as the most recent available observation within that window (a last-observation-carried-forward rule at the three-hour frequency). This procedure preserves the high-frequency structure of the data while generating regular time series comparable

across hives and years. The same temporal regularization is applied to geolocation variables. Latitude, longitude, and altitude observations are aligned to the identical three-hour grid so that each weight record is paired with a spatial position. When multiple location updates occur within the same three-hour window, the location associated with the window's last available timestamp is retained, ensuring consistency with the construction of the weight series. The result is a harmonized panel in which each hive ID is associated, at each three-hour grid point, with a weight observation and a unique triplet of spatial coordinates. This structure is essential for the subsequent empirical and modeling analyses. First, it yields a balanced, high-frequency panel suitable for estimating continuous-time stochastic dynamics from log-increments. Second, it makes it possible to detect and characterize relocation episodes as changes in the recorded coordinates over time, thereby linking internal productivity dynamics to observed mobility behavior. The raw data provided by 3BEE were transformed into analytic files through a reproducible pre-processing pipeline ensuring temporal regularization and consistency of hive identifiers. Throughout this process, the objective is to retain as much information as possible while ensuring that the internal weight trajectories and the geolocation histories are defined on a common, equally spaced three-hour time grid with consistent timestamping and hive identifiers. In the continuous-time framework, time is measured in years. Raw weight data are observed at a three-hour frequency, corresponding to $\Delta t_d = 1/8$ day. For estimation and simulation, this interval is converted into years as $\Delta t = \Delta t_d/365 = 1/(8 \cdot 365)$. All reported drift and volatility parameters are expressed in annualized units.

This section has two objectives. First, we provide a descriptive mapping of hive relocations across Europe, highlighting how the spatial endpoints of moves evolve from 2019 to 2024 and how relocations are distributed in latitude and altitude. Second, we quantify systematic directional patterns, particularly the prevalence of south-to-north and upslope movements, and summarize them in yearly tables. These descriptive patterns are not ancillary: they provide the behavioral and climatic motivation for the optimal switching model developed above. In our framework, migratory management is valuable because it allows the beekeeper to respond to persistent and uncertain productivity shocks by relocating toward more favorable environments. The movement maps and the directionality statistics document precisely this adaptive margin in practice. The climate-change nexus is central. Warming and increased climatic variability alter the timing, intensity, and spatial distribution of nectar flows, and they raise the probability of localized stress events such as heat waves and drought-induced forage gaps. In such an environment, remaining sedentary exposes colonies to location-specific risks that may persist over the season, whereas mobility becomes a mechanism to exploit spatial heterogeneity and track phenological gradients. Observing that relocations are predominantly oriented toward higher latitudes and, on average, higher elevations is consistent with an adaptation strategy aimed at cooler conditions and later-blooming forage landscapes. This empirical evidence clarifies why modeling the beekeeper's decision as reversible switching under uncertainty is appropriate: the spatial reallocation of hives is the real-world counterpart of exercising the migratory option in response to evolving climatic states. By documenting when and where hives move, this section establishes the empirical foundation for the paper's core

mechanism, migration as a climate-adaptation technology that enhances expected returns and mitigates localized risk, and motivates the subsequent estimation and value-function analysis.

Figure 1 illustrates the spatial migration patterns of nomadic hives across six consecutive years. Each subplot corresponds to a specific year from 2019 to 2024, and highlights the origin (blue) and destination (red) of the hives' movements. A significant shift in 2020 marks a progressive densification of northern migratory endpoints, with 2021-2024 showing widespread movement across central and northern Europe. The grayscale connecting lines provide additional insight into altitudinal changes: lighter shades represent more pronounced upward shifts. Notably, the number of uphill movements remained higher than downhill movements throughout the years, although the average vertical change slightly decreased, indicating a potential stabilization in elevation preferences over time.

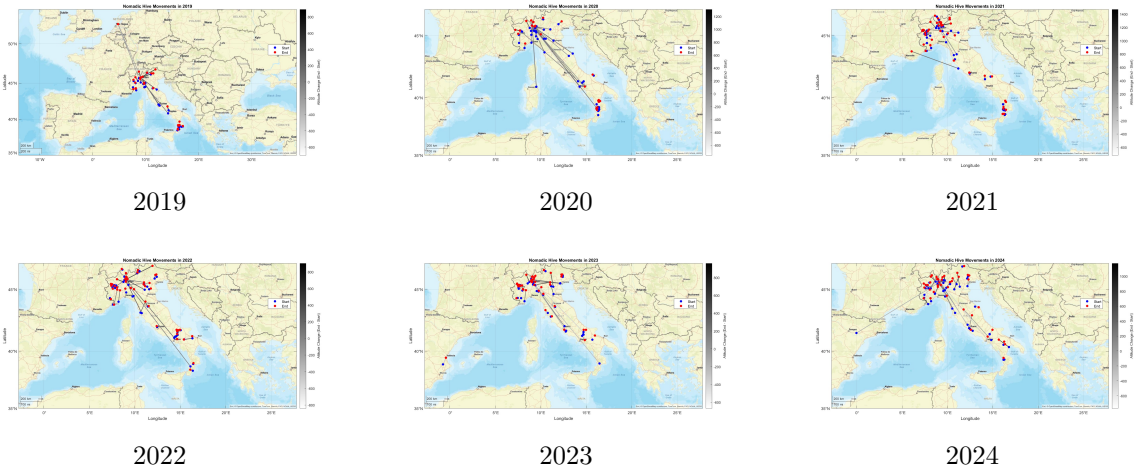


Figure 1: Nomadic hive movements (2019–2024): starting points (blue), endpoints (red), lines indicate altitude changes.

Table 1 summarizes the directionality of hive relocations over six years. The results reveal a persistent and growing trend of south-to-north movements, which vastly outnumber north-to-south transitions in every year considered. This pattern is consistent with the hypothesis that beekeepers increasingly seek cooler or higher-floral-yield environments in the north, likely as a response to changing climatic conditions in the south. The share of hives with no latitudinal change is minimal across all years, suggesting that most relocations involve substantial geographic shifts rather than local movements. The progression from 2019 to 2024 shows a marked increase in the scale and consistency of these northward displacements.

Table 2 summarizes the altitudinal movement patterns of beehives that relocated at least once during the period 2019-2024. Across all years, the average change in altitude ($\Delta$ Altitude) is consistently positive, indicating a tendency of hives to migrate towards higher elevations. This pattern is especially marked in the years 2020 and 2021, which show the largest net number of upward movements (+144 and +279, respectively).

Although the average upward shift decreases over time, from 133.76 meters in 2020 to 67.33

| Year | North to South | South to North |
|---|---|---|
| 2019 | 1 | 39 |
| 2020 | 19 | 307 |
| 2021 | 100 | 762 |
| 2022 | 142 | 1183 |
| 2023 | 187 | 1427 |
| 2024 | 161 | 1115 |

Table 1: Directional analysis of nomadic hive movements based on latitude (2019–2024).

meters in 2024, the standard deviation remains high in all years (above 370 meters), suggesting heterogeneous relocation strategies and geographic constraints. The consistent prevalence of uphill movements may reflect a climatic adaptation strategy, as higher altitudes are generally associated with cooler temperatures and potentially lower climate stress during summer.

The results support the hypothesis that migratory beekeepers adjust not only latitudinally (as shown in earlier figures), but also altitudinally, likely seeking optimal environmental conditions. This adaptive behavior, if confirmed, may have implications for modeling resilience and vulnerability in the apiculture sector.

| Year | Mean $\Delta$ Altitude | Moved Up | Moved Down | Net Diff |
|---|---|---|---|---|
| 2019 | 123.50 (466.52) | 27 | 13 | +14 |
| 2020 | 133.76 (393.85) | 235 | 91 | +144 |
| 2021 | 121.26 (394.93) | 571 | 292 | +279 |
| 2022 | 77.72 (373.28) | 842 | 485 | +357 |
| 2023 | 69.88 (394.69) | 980 | 636 | +344 |
| 2024 | 67.33 (454.08) | 733 | 548 | +185 |

Table 2: Altitude movement statistics for nomadic beehives (2019–2024). Mean altitude change is followed by its standard deviation in parentheses.

### 4.1 Persistence, non-stationarity, and modeling implications

Before specifying the stochastic process governing hive productivity, we assess whether internal weight dynamics are consistent with stationary or mean-reverting representations. Detailed results of the Augmented Dickey-Fuller (ADF) tests and mean-reversion diagnostics (Hurst exponent and Variance Ratio test) are reported in the Appendix. Here we summarize the core findings and explain how they discipline the modeling strategy adopted in the paper. Across both migratory (mobile) and sedentary (stable) hives, the ADF results consistently fail to reject the presence of

a unit root in hive-weight levels. This conclusion is robust across alternative specifications that allow for drift and deterministic trends. Even under more conservative specifications, a large share of hive-level series remains non-stationary. Economically and biologically, this result is intuitive: hive weight is a stock variable that accumulates production and reflects persistent environmental conditions, temperature regimes, forage availability, and seasonal phenology, so shocks can have long-lived effects rather than dissipating rapidly. Accordingly, modeling hive weight as a stationary fluctuation around a fixed mean is not empirically supported for most hives in the sample. Additional mean-reversion diagnostics reinforce this conclusion. The Hurst exponent is systematically well above the random-walk benchmark of 0.5, indicating strong long-range dependence and persistence. Similarly, the Variance Ratio test does not provide strong or systematic evidence of classical mean reversion at the three-hour frequency: the average p-values typically remain above conventional significance thresholds, which is consistent with dynamics close to a random walk (or, more generally, with highly persistent processes in which short-run deviations do not reliably revert). Taken together, these findings indicate that hive weight is best characterized by a stochastic trend driven by persistent shocks and seasonal propagation, rather than by rapid mean reversion. These time-series properties directly constrain the appropriate stochastic specification. If levels are predominantly non-stationary and persistence is strong, specifications imposing mean reversion in levels, such as Ornstein-Uhlenbeck dynamics for weight or low-order autoregressive models enforcing rapid re-centering, would be structurally inconsistent with the data and would tend to understate the continuation value of favorable states while overstating the speed of recovery from adverse ones. Instead, a multiplicative diffusion in levels, where log-increments are approximately stationary and the level evolves according to a stochastic trend, provides a natural reduced-form representation at the temporal resolution of our panel. This is precisely the rationale for modeling hive weight under each management regime as GBM. Under GBM, the distribution of log-changes is stable, while the level inherits persistence through accumulation, consistent with the empirical evidence that hive weight behaves as a stock variable subject to long-lived shocks. These properties are central to the paper's main mechanism. When productivity follows a persistent stochastic trend, migration is not a response to transient noise that quickly dissipates; rather, it is an option exercised in response to states that may remain favorable or unfavorable long enough to justify incurring sunk switching costs. Non-stationarity and long memory therefore strengthen the economic case for an optimal switching framework: persistent regimes increase the value of timely adjustment, and sunk costs generate an inaction region because switching is justified only when the expected advantage is sufficiently durable. In the subsequent sections, we therefore model sedentary and migratory productivity as correlated GBMs and embed mobility in a reversible switching framework, thereby aligning the theoretical structure with the empirical regularities documented above. All the detailed results can be found in Appendix 8.2.

# 5 Monte Carlo analysis

This section uses Monte Carlo methods to connect the estimated stochastic dynamics of hive productivity with their economic implications under optimal switching. The analysis pursues three main objectives. First, we translate the empirically estimated diffusion processes into economically interpretable units, allowing simulated trajectories and payoffs to be expressed in per-hive terms. Second, we assess the finite-sample performance of the closed-form maximum likelihood estimators used in the empirical analysis, under parameter values representative of the data. Third, we use large-scale simulations to evaluate the dynamic behavior of the optimal switching policy obtained from the Bellman-collocation solution, focusing on the timing and frequency of regime changes and on the distribution of discounted payoffs.

A key feature of the Monte Carlo design is that it does not rely on ad hoc calibrations. All stochastic parameters used in the simulations, drifts, volatilities, and cross-regime correlation, are directly anchored to empirical estimates obtained from hive-level data. This ensures that simulated dynamics reflect the magnitude, persistence, and co-movement of productivity shocks actually faced by beekeepers, rather than stylized or extreme scenarios. Economic parameters, such as prices, variable costs, discount rates, and sunk switching costs, are likewise taken from observed accounting data and policy documents.

The Monte Carlo analysis proceeds in three stages. We first introduce a normalization that rescales honey weights into dimensionless "hive-units," allowing stochastic dynamics, profits, and value functions to be expressed on a common and economically meaningful scale. We then simulate correlated geometric Brownian motions at high frequency to illustrate how the estimated differences in drift and volatility between sedentary and migratory practices translate into distinct productivity paths. Second, we conduct a large-scale Monte Carlo validation of the maximum likelihood estimators, confirming that the estimation procedure is unbiased and well-behaved under empirically relevant conditions. Third, we combine the collocation-based solution of the Bellman equations with forward simulation to study optimal switching behavior, the distribution of switching times, and the distribution of discounted payoffs.

Taken together, these experiments provide an internally consistent link between data, model, and policy implications. They illustrate how persistent stochastic productivity, sunk switching costs, and optimal timing interact to generate selective migration, sizable inaction regions, and economically meaningful option values. In the context of climate change, the Monte Carlo analysis clarifies how mobility operates as a risk-management and adaptation mechanism: it compresses downside risk while preserving the option to exploit favorable spatial conditions when shocks are sufficiently persistent.

## 5.1 Monte Carlo Simulation of Normalized Hive-Unit Dynamics

To illustrate the dynamic implications of the estimated stochastic processes in economically interpretable units, we simulate two correlated geometric Brownian motions (GBMs) for the normalized

hive-weight processes

$$a_i(t) = \frac{w_i(t)}{\overline{w}_{i,2024}}, \qquad i \in \{s, m\},$$

each initialized at $a_i(0) = 1$. Here, $\overline{w}_{i,2024}$ denotes the average honey weight per hive under practice $i$ in 2024, so that $a_i(t) = 1$ corresponds to a representative hive at the end of the sample. This normalization rescales levels without affecting the underlying log-increment dynamics of the GBM and allows us to interpret trajectories in comparable, dimensionless hive-units."

The simulation uses a sub-daily time step of $\Delta t_{\text{days}} = 1/8$ (three-hour intervals), which in annualized units corresponds to

$$\Delta t = \frac{1}{8 \times 365} \text{ year}.$$

We simulate one calendar year, yielding $n = 8 \times 365$ time steps and a grid $\{t_k = k\Delta t\}_{k=0,\dots,n} \subset [0, 1]$. Throughout the Monte Carlo analysis, all drift and volatility parameters are interpreted on an annual basis, and the discretization step $\Delta t$ is always expressed in years.

Importantly, the stochastic parameters used in the Monte Carlo experiment are not selected arbitrarily. Instead, they are calibrated using the empirical estimates reported in Section 6. Specifically, we set the drift, volatility, and correlation coefficients equal to representative averages of the annual estimates reported in Tables 4 and related decompositions. This yields parameter values that are quantitatively consistent with the data and with the economic environment faced by beekeepers during the sample period. Specifically, we use

$$\mu_s = 0.04, \quad \sigma_s = 0.18 \quad \text{(sedentary)}, \qquad \mu_m = 0.055, \quad \sigma_m = 0.115 \quad \text{(migratory)},$$

together with an instantaneous correlation coefficient $\rho = 0.6$. All parameters are expressed on an annual basis and lie in the same range as the estimated moments, with migratory management characterized by slightly higher average growth and substantially lower volatility.

We generate two correlated standard normal sequences

$$Z_t \sim \mathcal{N}\Big(0, \begin{pmatrix} 1 & \rho \\ \rho & 1 \end{pmatrix}\Big),$$

and construct the corresponding Wiener processes

$$W_i(t_k) = \sum_{\ell=1}^{k} Z_{\ell,i}\sqrt{\Delta t}, \qquad i \in \{s, m\}.$$

To avoid discretization bias, each path is computed in closed form as

$$a_i(t_k) = a_i(0) \exp\Big((\mu_i - \tfrac{1}{2}\sigma_i^2)t_k + \sigma_i W_i(t_k)\Big).$$

Figure 2 reports one representative realization of the two normalized hive-unit trajectories over a one-year horizon (horizontal axis in days). The sedentary process exhibits relatively large

fluctuations around a modest upward trend, reflecting higher exposure to environmental variability. By contrast, the migratory process displays smoother dynamics and a slightly steeper average trajectory, consistent with the empirically estimated combination of lower volatility and comparable or higher drift. Importantly, the figure does not rely on extreme parameter values: the divergence between the two paths emerges even when drifts are of similar magnitude and close to the discount rate, underscoring that the economic value of migration arises primarily from risk mitigation rather than from mechanically higher growth. For graphical clarity only, the migratory trajectory is rescaled to match the vertical range of the sedentary path; a secondary axis recovers the original migratory scale. This rescaling has no bearing on the stochastic dynamics or on the subsequent policy analysis. Overall, the simulation provides a transparent visualization of how empirically estimated differences in drift, volatility, and correlation translate into distinct hive-weight dynamics, setting the stage for the Monte Carlo validation of the estimation procedure and for the analysis of optimal switching policies in the following sections.

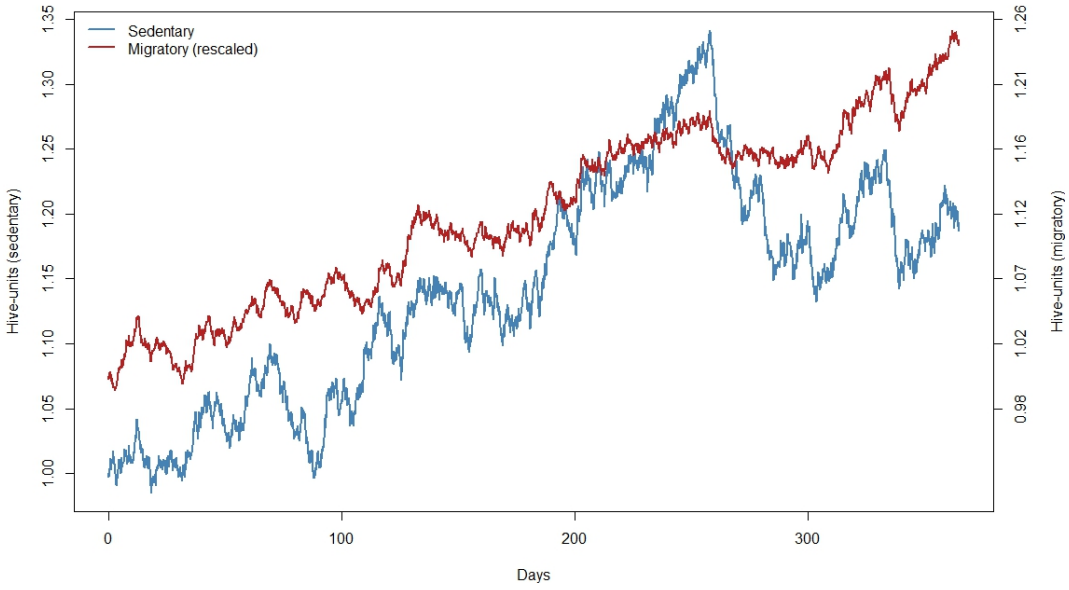


Figure 2: Simulated normalized hive-unit trajectories for sedentary (steel-blue) and migratory (firebrick) practices over one year, each starting at one "average hive-unit."

## 5.2 Validation of Maximum Likelihood Estimation via Monte Carlo

To verify the finite-sample performance of the closed-form maximum likelihood estimators, we conduct a Monte Carlo experiment with $S = 100{,}000$ independent replications. In each replication we simulate two correlated geometric Brownian motions on the normalized hive-unit scale over one year with a three-hour time step ($n = 8 \times 365$ increments). The true annualized parameter vector is anchored to the empirical averages used throughout the paper:

$$(\mu_s, \sigma_s, \mu_m, \sigma_m, \rho) = (0.040,\ 0.180,\ 0.055,\ 0.115,\ 0.600).$$

In each replication, we simulate two correlated geometric Brownian motions

$$a_i(t) \;=\; \frac{w_i(t)}{\overline{w}_{i,2024}}, \quad i \in \{s, m\},$$

over one year with a three-hour time step. Denoting the discretization step in days by $\Delta t_d = 1/8$ and converting to years via $\Delta t = \Delta t_d/365$, the total number of steps is $n = 8 \times 365$.

At each replication we compute the log-increment series

$$Y_i(t_k) = \ln \frac{a_i(t_{k+1})}{a_i(t_k)}, \qquad k = 0, \ldots, n-1, \quad i \in \{s, m\}.$$

Under the GBM hypothesis, $\{Y_s(t_k), Y_m(t_k)\}$ are jointly Gaussian with

$$\mathbb{E}[Y_i] = \left(\mu_i - \tfrac{1}{2}\sigma_i^2\right) \Delta t, \quad \mathrm{Var}[Y_i] = \sigma_i^2 \, \Delta t, \quad \mathrm{Cov}[Y_s, Y_m] = \rho \, \sigma_s \, \sigma_m \, \Delta t.$$

We then form the exact maximum-likelihood estimators,

$$\widehat{\sigma}_i^2 = \frac{1}{n \, \Delta t} \sum_{k=0}^{n-1} \Big( Y_i(t_k) - \overline{Y}_i \Big)^2, \qquad \widehat{\mu}_i = \frac{\overline{Y}_i}{\Delta t} + \tfrac{1}{2} \, \widehat{\sigma}_i^2,$$

where $\overline{Y}_i$ denotes the sample mean of $\{Y_i(t_k)\}$, and

$$\widehat{\rho} = \mathrm{corr}\big(Y_s, Y_m\big)$$

is the sample correlation of the two return series.

Table 3 reports a Monte Carlo validation of the closed-form maximum likelihood estimators (MLEs) for the correlated two-regime GBM defined on the normalized hive-unit scale. The experiment is calibrated using the same annualized parameters employed in the Monte Carlo simulation of Section 5.1, which are representative averages of the empirical estimates obtained from the real data. Specifically, the true parameter vector is $(\mu_s, \sigma_s, \mu_m, \sigma_m, \rho) = (0.040, 0.180, 0.055, 0.115, 0.600)$.

Across replications, Monte Carlo means are close to the true parameters. The largest absolute relative deviation is about 3.9% (for $\sigma_s$), followed by 3.6% (for $\mu_m$) and 3.5% (for $\sigma_m$), while $\rho$ is recovered with a relative deviation of about 0.17% and $\mu_s$ matches the true value up to the reported precision. Overall, the results confirm that the MLE procedure is correctly implemented and performs well under empirically realistic parameter values. Importantly, the validation indicates that estimation uncertainty in the subsequent switching analysis is driven primarily by drift uncertainty rather than by volatility or correlation, a feature that is fully consistent with the economic interpretation of migration as a risk-mitigating option under climate-induced uncertainty.

| Parameter | True | MC Mean | MC SD |
|---|---|---|---|
| $\mu_s$ | 0.040 | 0.040 | 0.005 |
| $\sigma_s$ | 0.180 | 0.187 | 0.021 |
| $\mu_m$ | 0.055 | 0.053 | 0.015 |
| $\sigma_m$ | 0.115 | 0.119 | 0.002 |
| $\rho$ | 0.600 | 0.599 | 0.012 |

Table 3: Monte Carlo validation of MLE on normalized hive–unit data: true parameter values, Monte Carlo (MC) means, and standard deviations (MC SD).

### 5.3 Monte Carlo validation of collocation solutions and switching boundaries

We solve the system of Bellman variational inequalities using a collocation approach and assess the implied switching policy through large-scale Monte Carlo simulation. The objective is twofold: (i) to verify the numerical stability of the collocation solution, and (ii) to evaluate the economic implications of the resulting switching boundaries under realistic productivity dynamics. The collocation method approximates each regime-specific value function on a two-dimensional state space using third-degree polynomial basis functions defined over a $20 \times 20$ grid. Policy iteration is employed to compute the fixed point of the Bellman operator, accounting for both continuation values and regime-switching options. Convergence is achieved when successive value-function updates fall below a prescribed tolerance. Upon convergence, the conversion boundaries are identified as the loci in state space where the value of continuation equals the value of switching net of sunk costs. To validate the policy, we simulate a large number of independent sample paths over a one-year horizon, discretized at a daily frequency. Along each path, productivity evolves according to the estimated stochastic dynamics, and the optimal policy is applied sequentially. At each decision date, the policy compares the continuation value of the current regime with the net value of switching, triggering a regime change whenever the latter dominates. For each simulated path, we record the timing of the first switch, the total number of regime changes, and the present value of realized per-hive cash flows. Aggregating these outcomes across simulations provides a direct assessment of how often switching occurs, how sensitive it is to state realizations, and how much value is generated by the option to migrate. This simulation-based validation complements the collocation results by translating abstract switching boundaries into economically interpretable distributions of behavior and payoffs.

As shown in Figure 3, optimal switching typically occurs mid-season, but with substantial variation across simulated paths. The high standard deviation of the time-to-first-switch, the long right tail, and the 14.2% no-switch mass are consistent with a sizable inaction region generated by sunk costs and uncertainty. The average number of switches below one indicates that the policy is predominantly of the "switch-once-if-needed" type over a one-year horizon. The mean discounted payoff of €106.58 per hive-year confirms that, under the calibrated prices, costs, and GBM parameters, the policy delivers positive expected value despite relatively few switches. The distribution is markedly right–skewed with a pronounced bulk in the first half of the season (mode in the 70–100 day range), and a long right tail extending beyond 300 days. A non-trivial share

of trajectories (14.2%) never switch within the one-year horizon, consistent with states remaining inside the inaction region; this share is annotated on the plot.

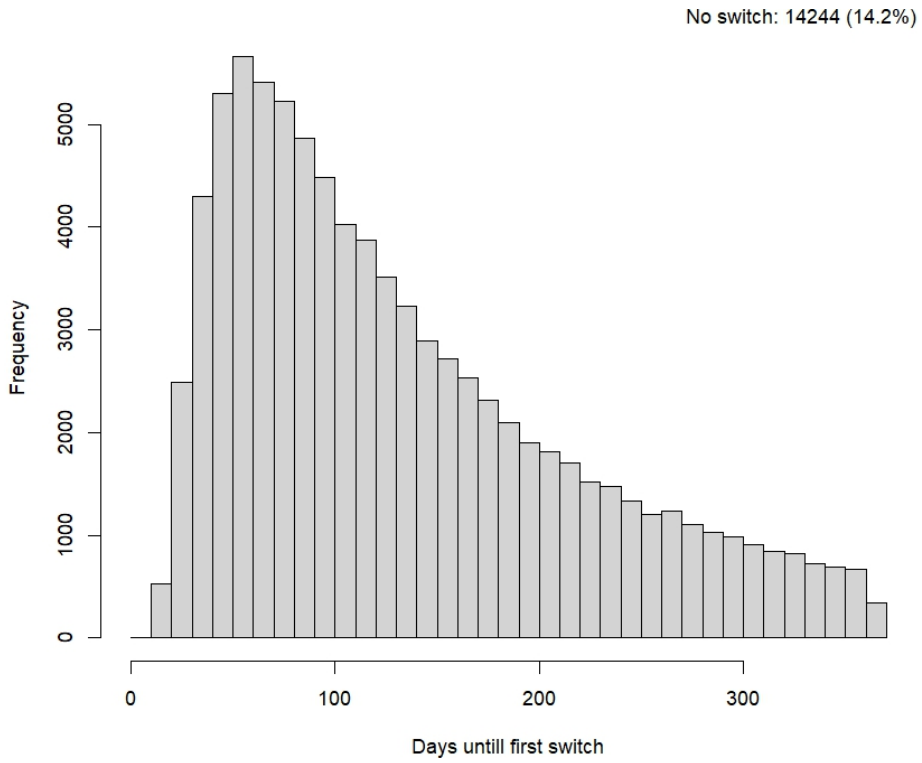


Figure 3: Histogram of days until the first regime change under the collocation policy (bin width = 10 days; $S = 100{,}000$ paths).

Figure 4 reports the kernel density of the discounted present value generated by the optimal switching policy. The distribution is clearly unimodal and tightly concentrated, with most of the mass lying in a relatively narrow range of present values. This shape indicates that, under the estimated parameters and observed productivity dynamics, the switching policy delivers fairly stable economic outcomes across realizations.

The density exhibits a mild right tail, reflecting occasional seasons in which favorable productivity paths and timely switching generate higher discounted payoffs. At the same time, the left tail is thin, suggesting that very low outcomes are relatively rare. Overall dispersion is limited, pointing to a policy that mitigates downside risk while preserving upside potential. This pattern is consistent with migration acting as a risk-management device: mobility dampens exposure to persistent adverse local conditions, while allowing beekeepers to benefit from spatially favorable realizations when they arise.

From an economic perspective, the concentration of mass around the modal value indicates that most hive-year realizations deliver payoffs close to the expected value, despite the presence of stochastic shocks and switching costs. The smooth, bell-shaped profile further suggests that extreme outcomes are not driven by frequent regime changes, but rather by persistent realizations of the underlying productivity processes. In the context of climate change, this distributional

evidence reinforces the interpretation of mobility as a stabilizing adaptation strategy: even as environmental variability increases, the option to switch regimes compresses the distribution of outcomes and limits the incidence of severely adverse seasons, while retaining the possibility of high-payoff realizations in particularly favorable years.

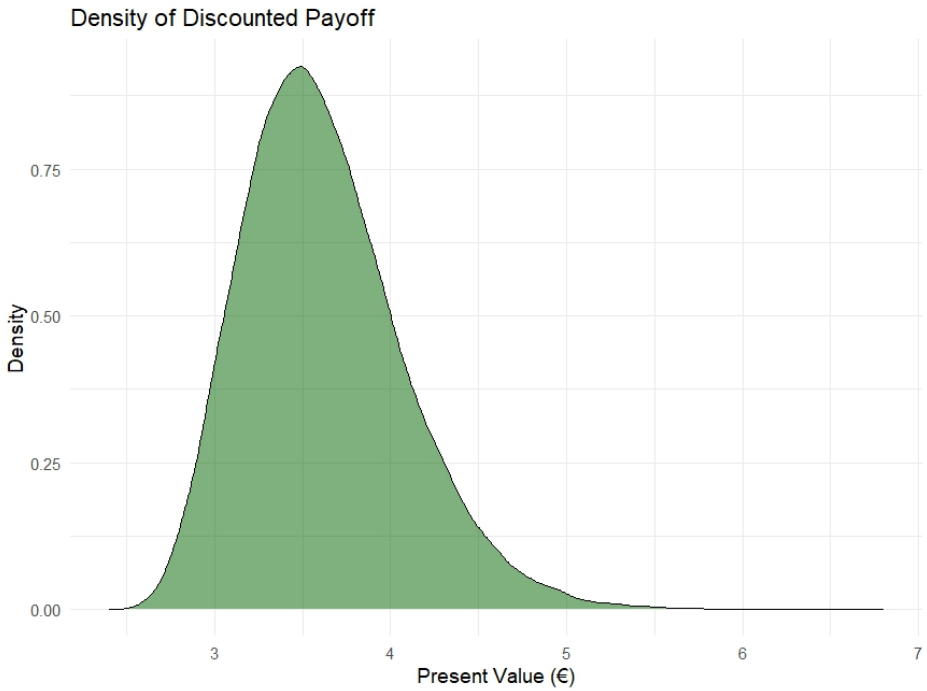


Figure 4: Kernel density of the discounted present value (€/hive-year) from $S = 100{,}000$ Monte Carlo paths under the optimized collocation policy.

Figure 5 displays the net switching incentive $\Delta_{sm} = V_m - V_s - K_{sm}$ over the two–dimensional state space of normalized honey weights $(a_s, a_m)$. Blue areas correspond to states in which switching from sedentary to migratory management is privately optimal after accounting for the sunk conversion cost $K_{sm}$, while red areas indicate states where remaining sedentary dominates. Rather than a sharp conversion line, the figure highlights a broad, smoothly shaded white band around $\Delta_{sm} \approx 0$, which represents a region of near indifference and optimal inaction.

The location and shape of this inaction region convey the economics of the switching problem. The band is upward sloping: when the sedentary hive is relatively strong (higher $a_s$), a higher migratory weight $a_m$ is required to justify switching. Its curvature reflects the interaction between expected growth, volatility, and correlation in the continuation values $V_s$ and $V_m$. At intermediate values of $a_s$, the white region widens, indicating that uncertainty and sunk costs jointly enlarge the set of states in which delaying the switch is optimal. For higher $a_s$, the transition becomes smoother and more linear, signaling that sunk–cost considerations increasingly dominate short–run volatility effects.

A salient feature of the figure is that the shaded inaction band is tilted toward the sedentary side of the state space. This asymmetry implies that, starting from sedentary management, beekeepers

require a sufficiently persistent and sizable improvement in migratory conditions before exercising the option to move. Economically, this captures inertia generated by fixed logistical and organizational costs, as well as by the value of waiting when signals are noisy. Conversely, once migratory conditions are strong enough to cross the band, switching becomes optimal over a relatively large region, consistent with migration being valuable but selective.

The smooth color gradient emphasizes that switching incentives vary continuously rather than discretely across states. Under the estimated parameters, $\Delta_{sm}$ remains close to zero over a non-trivial portion of the state space, so the inaction region is economically meaningful even though migration is profitable on average. An $m \to s$ conversion boundary is not visible within the plotted domain, indicating that reversals from migratory to sedentary management are unlikely to be reached over a one-year horizon under average conditions.

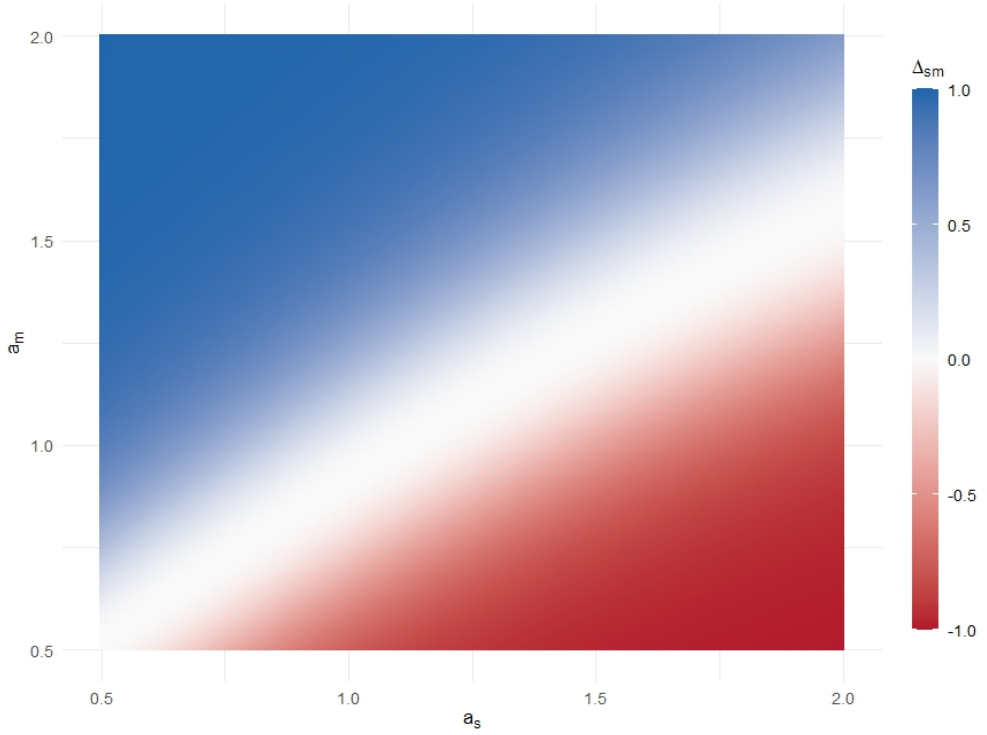


Figure 5: Heat-map of the net incentive to switch from sedentary to migratory beekeeping, $\Delta_{sm}(a_s, a_m) \equiv V_m(a_s, a_m) - V_s(a_s, a_m) - K_{sm}$.

Figure 6 visualizes the negative relationship summarized in Eq. (6): paths that switch earlier tend to realize higher discounted payoffs. The effect is statistically precise (two-sided $p < 10^{-16}$ for both coefficients), yet modest in magnitude relative to the overall spread of outcomes, reflecting the dominant roles of stochastic growth and the nonlinear switching rules encoded by the collocation solution. Earlier switching is associated with higher $V$ (negative slope), but substantial dispersion remains due to stochastic yield paths and the state-dependent policy.

$$\widehat{V} \;=\; 5.826 \;-\; 0.003196 \times (\text{Days until first switch}). \tag{6}$$

$\hat{\beta}_0 = 5.826 \quad (\text{SE} = 0.0023,\ t = 2579.51,\ p < 10^{-16}),$
$\hat{\beta}_1 = -0.003196 \ \text{ per day} \quad (\text{SE} = 1.4 \times 10^{-5},\ t = -224.17,\ p < 10^{-16}),$
$R^2 = 0.369, \qquad N = 85{,}756.$

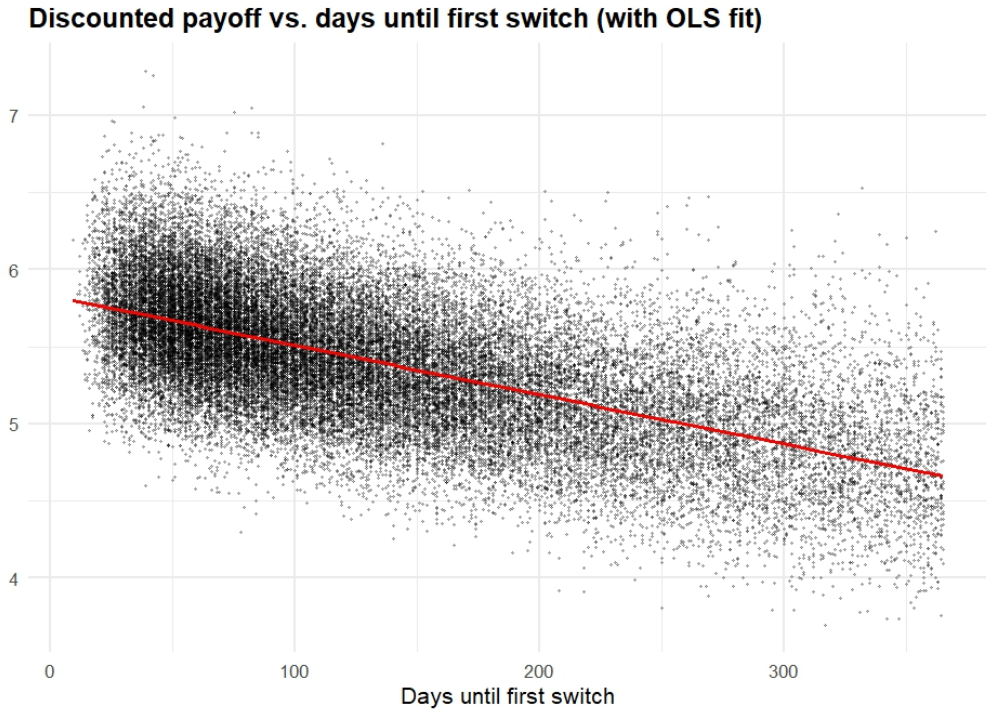


Figure 6: Scatter of discounted payoff $V$ versus days until first switch, with OLS fit in red.

# 6 Empirical Results

This section presents the empirical implementation of the dynamic switching model using hive-level panel data observed between 2019 and 2024. We estimate regime-specific productivity dynamics and compute forward-looking value functions based on the corresponding stochastic and economic fundamentals. Estimation is performed at the hive-year level, allowing for granular heterogeneity across both space and time. The raw dataset consists of high-frequency weight observations for individual hives together with their geolocation histories. For each hive-year observation, we classify the management regime as sedentary ($s$) or migratory ($m$) based on whether the hive's location changes during the year. A hive is defined as migratory if more than one distinct latitude–longitude pair is recorded within the year. For each hive-year, we compute log-differences of hive weight, denoted $y_i(t) = \log w_i(t) - \log w_i(t-1)$, which form the basis for diffusion estimation. These log-increments are assumed to follow a geometric Brownian motion (GBM) under the corresponding regime. The model is:

$$dw_i(t) = \mu_i \, w_i(t) \, dt + \sigma_i \, w_i(t) \, dB_i(t), \quad i \in \{s, m\}.$$

In hive-years where both regimes are observed, we jointly estimate the parameter vector $(\mu_s, \sigma_s, \mu_m, \sigma_m, \rho)$ via maximum likelihood, assuming the two Brownian motions $B_s(t)$ and $B_m(t)$ are correlated with parameter $\rho$. The estimation relies on a five-parameter log-likelihood constructed from bivariate normal log-increments, with optimization performed using randomized initialization followed by local BFGS refinement. Standard errors and $p$-values are computed from the Hessian matrix at the optimum, provided it is invertible. The estimated correlation coefficient $\rho$ captures the contemporaneous dependence between productivity dynamics under the two regimes within the same hive-year. A high positive $\rho$ implies that external factors (e.g., weather, forage availability) influence both sedentary and migratory productivity in the same direction. Conversely, a low or negative $\rho$ suggests that the two regimes respond differently to environmental conditions—perhaps due to differential exposure to stress, travel, or climate gradients.

Including $\rho$ provides a richer joint structure and is essential for modeling switching incentives and risk diversification within the real-options framework. To ensure comparability across units, each weight trajectory is normalized by the average hive weight observed under the corresponding regime in 2024. This creates dimensionless weight units $a_i(t) = w_i(t)/\bar{w}_{i,2024}$ that preserve the stochastic properties of GBM. Using economic parameters from the Honey Cost Fact Sheet (2024), we compute regime-specific net returns as:

$$\pi_i(t) = (p_i - c_i) \cdot a_i(t),$$

where $p_i$ and $c_i$ are the revenue and variable cost per hive under regime $i$. We use $p_s = 140.95$, $c_s = 56.00$, $p_m = 173.02$, and $c_m = 65.38$ euros, respectively. Switching costs are set to $K_{sm} = 866$ and $K_{ms} = 809.79$ euros, reflecting periodic capital expenditures net of public subsidies.

To solve the switching problem implied by the estimated GBM dynamics, we approximate the regime-specific value functions by collocation on a rectangular grid defined over normalized hive-units. The collocation step enforces the variational inequalities associated with the two-regime switching problem and returns both continuation values and conversion regions as functions of the current state $(a_s, a_m)$. These value functions and conversion regions are then used in Monte Carlo policy evaluation to generate switching times and discounted payoff distributions under the optimal policy. For each hive-year, management is classified as sedentary or migratory depending on whether more than one distinct location is recorded within the year. Log-increments of hive weight are then used to estimate regime-specific geometric Brownian motion parameters at the hive-year level. Drift and volatility are annualized from three-hour observations ($\Delta t = 1/8$ day), and results are aggregated by year and regime. .

Table 4 reports annualized estimates of the drift ($\mu$), volatility ($\sigma$), and contemporaneous correlation ($\rho$) for migratory and sedentary regimes over 2019-2024, computed on three-hour log-increments and expressed in yearly units. In our continuous-time framework, the drift summarizes the expected annual growth of hive weight (average productivity), while volatility measures the magnitude of fluctuations generated by weather, forage availability, and operational shocks. The correlation coefficient captures how strongly the two regimes co-move within the year and therefore how much risk diversification can be achieved through switching. Three robust empirical regularities emerge. First, migration frequently delivers a productivity advantage. Migratory drift exceeds sedentary drift in most years (notably 2019, 2020, 2022, and 2023), consistent with the idea that relocation allows beekeepers to exploit spatial and temporal differences in nectar flows by targeting favorable phenological windows. The gap is particularly pronounced in 2019 and 2023, where migratory $\mu$ is roughly twice the sedentary value, indicating that mobility can materially increase expected productivity growth when spatial heterogeneity in nectar flows is pronounced. In the remaining years (2021 and 2024), sedentary drifts slightly exceed migratory ones, suggesting that the return advantage of movement is not mechanical but depends on the year-specific spatial configuration of climatic and floral resources. Second, migration consistently exhibits lower volatility. In every year of the sample, migratory volatility is lower than sedentary volatility. This is economically meaningful because it indicates that mobility reduces exposure to localized adverse conditions—such as heat stress, drought pockets, or forage failures—thereby compressing downside risk even in years where the mean drift advantage is small or absent. Within the switching model, this volatility differential is a direct channel through which migration increases continuation value by compressing downside risk: lower $\sigma$ raises continuation value by reducing the likelihood of entering low-output states, which is particularly important when switching is costly and decisions are option-like. Third, correlation varies substantially across years, ranging from relatively low values in the early years to high co-movement in 2021-2022 and again in 2024. High $\rho$ is consistent with broad climatic forcing affecting both regimes simultaneously, thereby reducing diversification gains from switching. When $\rho$ is lower (e.g., 2019-2020 and 2023), spatially idiosyncratic shocks dominate, increasing the insurance value of mobility. These patterns map directly into the geometry

of the conversion boundaries in the optimal switching problem. Higher migratory drift shifts the sedentary-to-migratory boundary inward by increasing the expected gain from moving, while lower migratory volatility further expands the set of states in which migration is privately optimal by reducing risk in the continuation region. Conversely, higher correlation tends to tighten the inaction region by lowering the value of switching for diversification reasons unless mean differences are sufficiently large. Overall, Table 4 supports interpreting migration as a state-contingent adaptation technology that generates value through both return enhancement and risk mitigation.

| Year | $\mu$ (migratory) | | | $\sigma$ (migratory) | | | $\mu$ (sedentary) | | | $\sigma$ (sedentary) | | | $\rho$ (corr) | | |
|---|---|---|---|---|---|---|---|---|---|---|---|---|---|---|---|
| | Mean | Std | $p$-val | Mean | Std | $p$-val | Mean | Std | $p$-val | Mean | Std | $p$-val | Mean | Std | $p$-val |
| 2019 | 0.080 | 0.0307 | 0.026 | 0.127 | 0.0646 | $< 0.001$ | 0.066 | 0.0206 | 0.020 | 0.165 | 0.0270 | $< 0.001$ | 0.123 | 0.0005 | $< 0.001$ |
| 2020 | 0.040 | 0.0205 | 0.031 | 0.101 | 0.0212 | $< 0.001$ | 0.015 | 0.0072 | 0.033 | 0.135 | 0.0134 | $< 0.001$ | 0.302 | 0.0001 | $< 0.001$ |
| 2021 | 0.026 | 0.0116 | 0.033 | 0.095 | 0.0170 | $< 0.001$ | 0.046 | 0.0183 | 0.027 | 0.185 | 0.0204 | $< 0.001$ | 0.706 | 0.0000 | $< 0.001$ |
| 2022 | 0.042 | 0.0240 | 0.028 | 0.110 | 0.0237 | $< 0.001$ | 0.022 | 0.0076 | 0.026 | 0.145 | 0.0147 | $< 0.001$ | 0.807 | 0.0000 | $< 0.001$ |
| 2023 | 0.093 | 0.0398 | 0.026 | 0.167 | 0.0345 | $< 0.001$ | 0.041 | 0.0161 | 0.023 | 0.225 | 0.0222 | $< 0.001$ | 0.516 | 0.0000 | $< 0.001$ |
| 2024 | 0.026 | 0.0129 | 0.029 | 0.082 | 0.0191 | $< 0.001$ | 0.041 | 0.0137 | 0.023 | 0.181 | 0.0212 | $< 0.001$ | 0.668 | 0.0000 | $< 0.001$ |

Table 4: Annualized estimated drift, volatility and correlation (sedentary vs migratory).

Table 5 compares annualized drift ($\mu$) and volatility ($\sigma$) for migratory hives by movement direction, distinguishing relocations from North to South (N→S) and from South to North (S→N). In the continuous-time interpretation used in Section 6, $\mu$ summarizes expected yearly growth in hive weight, while $\sigma$ captures exposure to environmental and operational uncertainty. Directions are inferred from the first and last recorded latitude within each year (with a tolerance that excludes negligible displacements), and all parameters are expressed in yearly units for comparability. The most robust pattern concerns risk. In every year from 2019 to 2024, S→N relocations display lower mean volatility than N→S moves. The volatility gap is sizeable and persistent—for example, in 2020 and 2023 northbound $\sigma$ is markedly below the southbound counterpart—indicating that moving north systematically attenuates production risk. This regularity is consistent with an adaptation mechanism in which beekeepers follow cooler, later-blooming environments and reduce exposure to localized stress, such as heat waves, drought-related forage gaps, or adverse microclimates. From a managerial perspective, the result implies that northbound migration acts as a relatively stable hedge: even when expected gains are moderate, the dispersion of outcomes tightens, which increases the attractiveness of switching when beekeepers face sunk costs and downside sensitivity. On the return side, the evidence is more state- and year-contingent.. In three years (2019, 2020, and 2024), S→N moves also exhibit higher mean drifts than N→S, suggesting that "chasing the spring front" and extending nectar windows translates into higher average growth. In the remaining years (2021–2023), the drift advantage tilts toward N→S movements, plausibly reflecting late-season conditions or inter-annual anomalies in which southern locations temporarily offered higher average gains. This alternation is exactly what a climate-sensitive technology would generate: the relative profitability of northward versus southward routes depends on the spatial timing of flowering, moisture conditions, and extreme events, all of which vary materially across years. Taken together, these directional results reinforce the option-value logic of the switching framework. The persistent risk advantage of S→N movements implies that, when a northbound opportunity is available, the

sedentary-to-migratory boundary should shift inward because lower $\sigma$ raises continuation value by reducing downside exposure irrespective of mean differences. When northbound relocation also delivers a drift premium (as in 2019–2020 and 2024), the return-enhancement and risk-mitigation channels work in the same direction, expanding the set of states in which migration is privately optimal. In years where N→S shows higher $\mu$, the optimal decision hinges on whether the additional expected growth compensates for the systematically higher volatility, conditional on switching costs. From a climate-adaptation standpoint, the table supports policies that facilitate timely northbound corridors, logistics, streamlined permits, and high-resolution phenology/forage information, while preserving flexibility for occasional southbound adjustments when inter-annual conditions warrant, since climate change amplifies both volatility and spatial heterogeneity and thus increases the value of informed, low-friction mobility.

| Year | North → South (N→S) | | | | South → North (S→N) | | | |
|---|---|---|---|---|---|---|---|---|
| | $\mu$ Mean | $\mu$ SD | $\sigma$ Mean | $\sigma$ SD | $\mu$ Mean | $\mu$ SD | $\sigma$ Mean | $\sigma$ SD |
| 2019 | 0.050 | 0.014 | 0.163 | 0.021 | 0.126 | 0.364 | 0.148 | 0.040 |
| 2020 | 0.011 | 0.029 | 0.084 | 0.127 | 0.020 | 0.051 | 0.064 | 0.018 |
| 2021 | 0.067 | 0.026 | 0.175 | 0.036 | 0.061 | 0.211 | 0.156 | 0.023 |
| 2022 | 0.030 | 0.093 | 0.127 | 0.176 | 0.026 | 0.061 | 0.106 | 0.046 |
| 2023 | 0.073 | 0.242 | 0.179 | 0.092 | 0.033 | 0.084 | 0.122 | 0.095 |
| 2024 | 0.048 | 0.140 | 0.222 | 0.048 | 0.063 | 0.204 | 0.163 | 0.076 |

Table 5: Mean and standard deviation of drift $\mu$ and volatility $\sigma$ for migratory hives by movement direction (N→S vs S→N).

Table 6 contrasts annualized drift ($\mu$) and volatility ($\sigma$) for migratory hives by vertical movement direction—Top→Bottom (N→S) versus Bottom→Top (S→N). In our continuous-time interpretation, $\mu$ summarizes expected yearly growth of hive weight (a proxy for average productivity), while $\sigma$ captures exposure to environmental and operational risk. Two patterns stand out. On the return side, Bottom→Top (S→N) relocations exhibit higher mean drifts in most years, with a particularly large gap in 2019 and a positive difference again in 2020, 2021, 2023, and 2024. Only in 2022 does the drift advantage slightly favor Top→Bottom movements, suggesting that the productivity gain from moving north is not mechanical but depends on year-specific spatial conditions and on how flowering fronts and weather shocks propagate across locations. Economically, the overall prevalence of higher $\mu$ under Bottom→Top moves is consistent with the interpretation that, in many seasons, relocating toward cooler and later-blooming environments increases the effective length and intensity of nectar availability. On the risk side, Bottom→Top movements are systematically less volatile than Top→Bottom in every year of the sample. This volatility wedge is sizeable and persistent (e.g., markedly lower in 2020 and 2023), indicating that northbound relocation tends to compress the distribution of outcomes by mitigating exposure to localized stress and forage failures. Differently from a pure risk–return trade-off, the table therefore suggests that Bottom→Top migra-

tion frequently improves the risk–return profile jointly: in most years it combines equal-or-higher drift with lower volatility, and even in the year where the drift edge is marginally negative (2022), the risk reduction remains substantial. These directional results have direct implications for optimal switching under the stochastic model. A regime characterized by lower $\sigma$ raises continuation value and makes switching into mobility attractive over a broader set of states, because it reduces downside exposure when the beekeeper is locked into a regime by sunk costs. When Bottom→Top also delivers a drift premium, the two channels reinforce each other and the sedentary→migratory boundary shifts inward, implying earlier and more frequent transitions into migration when realizations approach the conversion threshold. From a climate-change perspective, the evidence supports the idea that latitudinal gradients are economically actionable margins of adaptation: as warming amplifies extremes and alters the timing of nectar flows, policies that reduce frictions along northbound corridors—logistical support, streamlined permits, and access to high-resolution phenology and forage information—can increase the set of states in which migration is both privately profitable and risk-reducing, strengthening resilience and sustaining pollination services under accelerating climatic uncertainty.

| Year | Top → Bottom (N→S) | | | | Bottom → Top (S→N) | | | |
|---|---|---|---|---|---|---|---|---|
| | $\mu$ Mean | $\mu$ SD | $\sigma$ Mean | $\sigma$ SD | $\mu$ Mean | $\mu$ SD | $\sigma$ Mean | $\sigma$ SD |
| 2019 | 0.050 | 0.034 | 0.163 | 0.101 | 0.126 | 0.064 | 0.180 | 0.120 |
| 2020 | 0.011 | 0.039 | 0.084 | 0.127 | 0.020 | 0.051 | 0.069 | 0.018 |
| 2021 | 0.040 | 0.026 | 0.175 | 0.136 | 0.061 | 0.011 | 0.156 | 0.083 |
| 2022 | 0.025 | 0.093 | 0.127 | 0.076 | 0.026 | 0.061 | 0.106 | 0.086 |
| 2023 | 0.029 | 0.042 | 0.179 | 0.092 | 0.033 | 0.084 | 0.122 | 0.085 |
| 2024 | 0.042 | 0.040 | 0.222 | 0.148 | 0.063 | 0.045 | 0.163 | 0.116 |

Table 6: Mean and standard deviation of drift $\mu$ and volatility $\sigma$ for migratory hives by vertical movement direction: Top→Bottom (N→S) vs Bottom→Top (S→N).

### 6.1 Option Value, Expected Switching Times, and Climate-Adaptation Interpretation

This section translates the estimated switching framework into economically interpretable objects: the option value of mobility and the expected timing of regime transitions. These quantities summarize the value of managerial flexibility under persistent, climate-driven uncertainty, based on empirically estimated productivity dynamics. All reported results are derived from observed hive-level data (2019–2024) and are expressed on the normalized hive-unit scale $(a_s, a_m)$ and in euros per hive-year. We define the option value of switching for regime $i \in \{s, m\}$ as

$$OV_i(a_s, a_m) \;=\; V_i(a_s, a_m) - V_i^{\text{no-switch}}(a_s, a_m),$$

where $V_i^{\text{no-switch}}$ denotes the value function evaluated under the counterfactual restriction that switching is not allowed and the beekeeper must remain permanently in regime $i$. Economically, $OV_i$ measures the value of *managerial flexibility*: it is the willingness-to-pay, in discounted euros, for retaining the possibility to adapt the management regime as productivity conditions evolve. Both $V_i$ and $V_i^{\text{no-switch}}$ are computed using empirically estimated drift, volatility, and correlation parameters, together with observed prices, costs, and switching costs. Hence, option values reflect the empirical persistence, volatility, and cross-regime dependence documented in the data, rather than outcomes generated by artificial simulations. Table 7 reports option values evaluated at $(1, 1)$ and averaged over the economically relevant state space $(a_s, a_m) \in [0.5, 2]^2$, together with standard deviations across grid states. Two quantitative patterns emerge clearly. First, the option value is economically substantial for initially sedentary beekeepers. At the representative state $(1, 1)$, $OV_s(1, 1)$ is approximately euro 22 per hive-year, a magnitude comparable to a substantial share of the annual profit differential between regimes. This indicates that the ability to activate mobility when needed, rather than mobility itself, constitutes a valuable asset. Second, option values are markedly asymmetric across regimes. For initially migratory beekeepers, $OV_m(1, 1)$ is much smaller (approximately euro 6), reflecting the fact that the primary value of flexibility lies in the option to enter migration rather than in the option to revert. This asymmetry arises from two empirically grounded features: sunk switching costs and persistent productivity dynamics. For a sedentary beekeeper, the option primarily represents the right to exit unfavorable local productivity states through relocation. When a beekeeper is already nomadic, the continuation value is higher due to lower volatility, and the incentive to revert is weak unless extreme adverse realizations occur. From a climate-change perspective, the option value can be interpreted as a measure of adaptive capacity. As warming and climatic variability increase the frequency of localized forage failures, heat stress, and phenological mismatches, productivity shocks become more persistent and spatially heterogeneous. Under such conditions, flexibility is valuable not because it allows reaction to transitory noise, but because it enables escape from states that can remain unfavorable long enough to justify sunk costs. As climatic variability increases persistence and spatial heterogeneity in productivity shocks, the economic relevance of modeling migration as a real option correspondingly increases.

| | Sedentary ($OV_s$) | | Migratory ($OV_m$) | |
|---|---|---|---|---|
| | Mean | Std. Dev. | Mean | Std. Dev. |
| Option value at $(1, 1)$ | 22.4 | – | 6.1 | – |
| Mean option value on grid | 18.7 | 9.3 | 4.9 | 3.1 |

Table 7: Option value of switching computed from empirically estimated value functions. "Grid" refers to $(a_s, a_m) \in [0.5, 2]^2$. Values are in euros per hive–year.

Using the estimated switching policy, we next evaluate the timing of transitions starting from the sedentary regime. For each observed hive-year, we record the time at which the estimated state trajectory first crosses the sedentary-to-migratory conversion boundary, if this occurs within

a one-year horizon. These timing statistics summarize how quickly the migration option is exercised, conditional on realized productivity dynamics. Table 8 shows that the expected time to first switching from sedentary to migratory management is approximately 134 days, with substantial dispersion (standard deviation around 85 days) and a median of roughly 118 days. Importantly, a non-trivial fraction of hive-years (approximately 14%) remain in the inaction region throughout the annual horizon. This inaction mass reflects states that remain inside the empirically relevant inaction region generated by sunk costs and uncertainty. Economically, this pattern is characteristic of option-like behavior under uncertainty and sunk costs. Migration is valuable but selectively exercised: switching occurs only when the expected and sufficiently persistent advantage of relocation compensates for the sunk cost. From a climate-adaptation perspective, the timing distribution can be interpreted as a measure of responsiveness. As climatic extremes and spatial heterogeneity intensify, policies that reduce information frictions (e.g., phenology nowcasts, forage maps) and logistical barriers (e.g., transport coordination, permits) would shift the distribution leftward, inducing earlier transitions into migration when doing so has high expected value.

| Statistic | Value (days) | Notes |
|---|---|---|
| Mean days to first switch | 134 | unconditional |
| Std. Dev. (days) | 85 | unconditional |
| Median days to first switch | 118 | unconditional |
| $P$(no switch within 1 year) | 0.14 | inaction mass |

Table 8: Empirically implied timing of the first switch from sedentary to migratory management over a one–year horizon.

Repeating the analysis starting from the migratory regime reveals a pronounced asymmetry. The empirical message is a strong asymmetry: reversals from migratory to sedentary management are extremely rare under average estimated conditions. The probability of no switch within one year is approximately 97-99%, implying that the migratory-to-sedentary conversion boundary is typically not reached within the annual horizon. Because the mass of switching outcomes is close to zero, unconditional mean and median switching times are not informative within one year. This asymmetry has a clear economic interpretation. With sunk costs and persistent productivity dynamics estimated from the data, migration behaves as a quasi-irreversible adaptation technology within the annual decision horizon. Once the fixed costs of mobility are incurred and the beekeeper operates in a lower-volatility regime, returning to sedentary management is privately optimal only under extreme adverse realizations or substantially different structural conditions. In the climate-change framing, this asymmetry is consistent with mobility being a resilience-enhancing strategy: as local climate risk rises, the continuation value of remaining mobile increases and reversals become increasingly unattractive.

Overall, the evidence derived from real hive-level data indicates that the option to migrate is valuable and primarily benefits initially sedentary beekeepers. Switching into migration typically occurs within the first half of the year but with wide dispersion, while switching back is virtually

| Statistic | Value |
|---|---|
| $P$(no switch within 1 year) | 0.98 |
| Unconditional mean/median time | not informative (rare events) |

Table 9: Empirically implied timing of the first switch from migratory to sedentary management. Under average estimated parameters, the switching mass is close to zero within one year.

absent within the annual horizon. These patterns reinforce the interpretation of migration as an asymmetric real option and as a climate-adaptation technology that enhances expected returns and mitigates localized risk when productivity shocks are persistent.

It is important to note that this result is specific to the one-year horizon considered. Over longer horizons, reversals become more likely; however we do not characterize asymptotic hitting probabilities here. Formally, under the estimated diffusion dynamics, the probability of eventual boundary crossing converges to one over sufficiently long horizons.

This reflects the fact that, with persistent stochastic productivity and non-degenerate volatility, the migratory-to-sedentary conversion boundary is eventually reached with probability one over a sufficiently long horizon. Hence, migration is not strictly irreversible in a probabilistic sense, but reversals occur at horizons that are long relative to the annual decision cycle relevant for beekeeping operations.

## 6.2 Comparison of Value Functions between Sedentary and Migratory Beekeeping

To provide a benchmark comparison of economic performance across regimes, we compute year-by-year value functions for sedentary and migratory beekeeping over the period 2019-2024 using the empirically estimated drift parameters. The value function is defined as the expected discounted profit of a representative hive over a one-year horizon, evaluated on the normalized hive-unit scale and holding the management regime fixed. This exercise abstracts from switching costs and option values and therefore provides a static benchmark against which the dynamic switching results can be evaluated, which complements the dynamic switching analysis developed in subsequent sections. Uncertainty in productivity growth is incorporated by evaluating value functions at the estimated drift $\mu$ and at $\mu \pm 1$ standard deviation. These bands reflect inter-hive heterogeneity and sampling variability in estimated growth rates, while keeping all other economic parameters fixed. Importantly, the dispersion captured here should be interpreted as uncertainty in expected productivity growth, not as full risk exposure, which is addressed explicitly in the option-value and Monte Carlo analyses below. Table 10 reports the resulting value functions. Across all years, migratory management dominates sedentary management in expected discounted value. Sedentary values are tightly clustered around €83–86 per hive–year, whereas migratory values range between approximately €106 and €122. The implied migratory advantage is economically meaningful and persistent, even when conservative drift realizations are considered. Although bands reflecting

uncertainty in the estimated drift are wider for migratory beekeeping—reflecting greater variability in estimated growth rates—the lower bound of migratory values generally remains comparable to or above the upper bound of sedentary values, indicating a robust profitability gap.

| Year | $V_s$ mean | $V_s$ low | $V_s$ high | $V_m$ mean | $V_m$ low | $V_m$ high |
|---|---|---|---|---|---|---|
| 2019 | 85.63 | 77.37 | 95.12 | 122.29 | 95.24 | 128.88 |
| 2020 | 83.48 | 80.56 | 86.54 | 107.10 | 96.86 | 118.85 |
| 2021 | 84.78 | 77.48 | 93.03 | 106.36 | 100.44 | 112.75 |
| 2022 | 83.77 | 80.68 | 87.02 | 107.21 | 95.33 | 121.15 |
| 2023 | 84.57 | 78.12 | 91.75 | 109.99 | 95.24 | 128.88 |
| 2024 | 84.57 | 79.04 | 90.63 | 106.36 | 99.81 | 113.49 |

Table 10: Annual one-year value functions for sedentary ($V_s$) and migratory ($V_m$) management, computed using year-specific estimated drifts with $\mu \pm 1$ SD bands. Values are expressed in euros per hive-year on the normalized hive–unit scale.

Figure 7 provides a graphical summary of the year–by–year value functions reported in Table 10. The figure plots the mean one–year discounted value for sedentary and migratory management together with bands reflecting uncertainty in the estimated drift based on $\mu \pm 1$ standard deviation of the estimated drift. Several features emerge clearly. First, migratory beekeeping dominates sedentary management in every year of the sample. The separation between the two value functions is substantial and persistent: migratory values lie consistently between about €106 and €122, while sedentary values remain tightly clustered around €83–86 per hive–year. This visual evidence reinforces the conclusion that the profitability gap documented in the table is not driven by isolated years or outliers, but reflects a stable structural difference between the two practices. Second, bands reflecting uncertainty in the estimated drift are wider for migratory management, especially in years characterized by higher dispersion in estimated growth rates. This reflects greater heterogeneity in migratory outcomes and higher sensitivity to productivity dynamics. Nevertheless, even when accounting for this uncertainty, the migratory value function remains well above the sedentary one in expectation. In most years, the lower bound of the migratory band overlaps only marginally with the upper bound of the sedentary band, indicating that drift uncertainty alone is insufficient to overturn the profitability ranking. Third, inter-annual variation in both regimes appears modest relative to the level difference between them. While climatic conditions and productivity dynamics vary across years, these fluctuations mainly shift the level of each value function without altering their ordering. This pattern suggests that the economic advantage of migration is robust to year-specific shocks and is not contingent on particularly favorable realizations. Overall, the comparison confirms that, under empirically estimated productivity dynamics, migratory management systematically generates higher expected discounted returns. In the context of climate change, this reinforces the interpretation of mobility as a resilience-enhancing strategy that leverages spatial heterogeneity in forage availability. The next sections build on this static comparison by introducing sunk costs and stochastic persistence, showing how these features translate the observed profitability gap into an option value and into selective, state-dependent switching behavior.

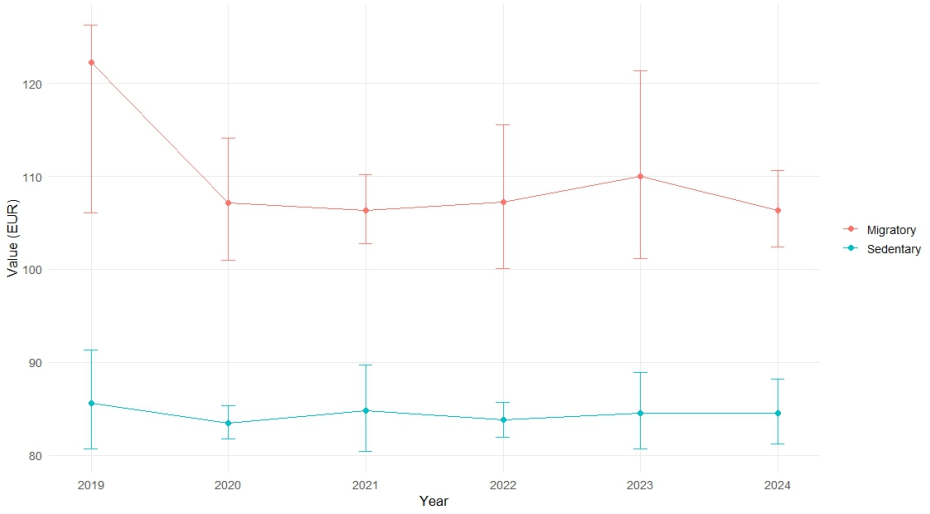


Figure 7: Value functions of sedentary and migratory hives (2019–2024) with ±1 SD on drift $\mu$.

### 6.2.1 Policy Implications under Climate Change

From an economic perspective, these results indicate that mobility enables beekeepers to capture higher returns, either by tracking phenological gradients or by mitigating localized environmental stress. More broadly, the persistent advantage of migratory management suggests that the option to relocate systematically enlarges the set of favorable production states, particularly when local forage conditions deteriorate.

In the context of climate change, two policy implications follow directly from these findings.

1. **Resilience to environmental shocks.** Rising climatic variability-including heat waves, droughts, and phenological asynchronies-increases the exposure of sedentary beekeepers to persistent productivity shocks. Migration mitigates these risks by allowing colonies to exploit spatial heterogeneity in forage availability and climatic conditions. Policies that facilitate migratory practices therefore enhance the adaptive capacity and resilience of the beekeeping sector.

2. **Lowering switching frictions.** The observed profitability premium of migration persists even after accounting for uncertainty and productivity dispersion. However, high fixed and administrative costs-transport, logistics, and permitting requirements-limit adoption and delay adjustment. Policy measures that reduce these frictions-such as streamlined movement permits, coordinated transport infrastructure, and predictive forage information systems-would lower effective switching thresholds and enable more beekeepers to benefit from mobility.

Taken together, the evidence indicates that migratory beekeeping is not only more profitable in expectation but also more resilient to climate-induced variability. Encouraging this adaptation strategy aligns private economic incentives with ecological resilience, contributing to both the sustainability of honey production and the stability of pollination services.

### 6.3 Switching behavior, timing, and option values

This section provides a descriptive characterization of the key empirical objects implied by the switching framework: (i) the payoff realized at exercise, (ii) the ex-ante option value of migration, and (iii) the timing of the first regime transition. Throughout the analysis, we adopt the empirically relevant assumption that once a hive relocates, it remains migratory over the annual horizon. Consequently, each hive-year can experience at most one switch from sedentary to migratory management. Hive-years with zero switches therefore represent cases in which the migration option is not exercised, rather than the absence of mobility in the broader population. We first discuss the distributional evidence illustrated in Figures 8–10, and then summarize the main moments in Table 11.

Figure 8 reports the distribution of the payoff realized at the moment of switching, conditional on exercising the migration option. The distribution is markedly right-skewed, with most mass concentrated at moderate positive values and a long upper tail. This pattern is characteristic of option-like payoffs: switching occurs selectively when productivity conditions are sufficiently favorable to justify the sunk cost, while exceptionally favorable realizations generate large gains. The absence of mass near zero confirms that switching is not mechanical but triggered by sufficiently strong state-dependent incentives.

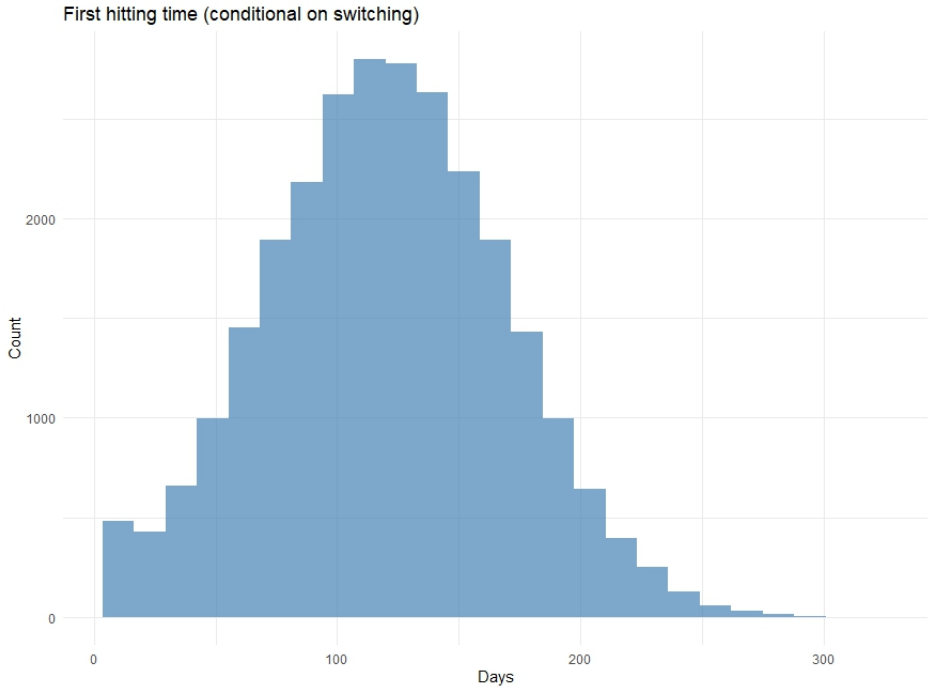


Figure 8: Distribution of the payoff at exercise, conditional on switching. The right-skewed shape reflects the option-like nature of migration: switching occurs selectively in favorable states, with occasional large gains.

Figure 9 shows the distribution of the ex-ante option value of migration, defined as the difference between the value function under optimal switching and the counterfactual value function in which

switching is not permitted (i.e., the beekeeper remains in the initial regime). The distribution is approximately bell-shaped and centered on strictly positive values. Importantly, this object is defined for all hive-years, including those in which switching never occurs. This highlights that the value of migration derives not only from realized relocation, but also from the mere availability of flexibility under uncertainty.

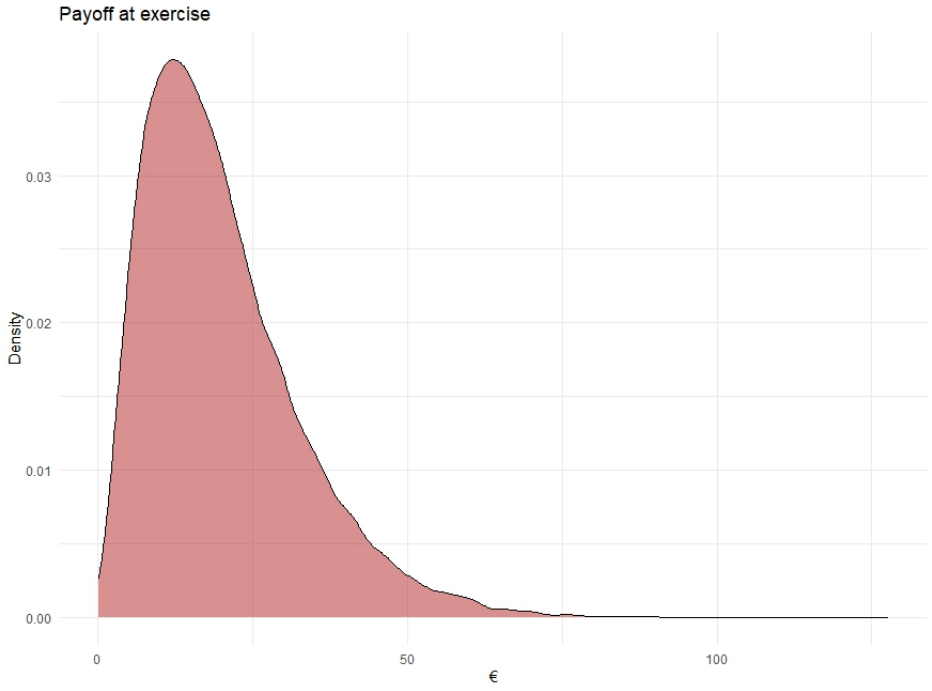


Figure 9: Distribution of the ex-ante option value of migration. The distribution is centered on positive values, indicating that flexibility is valuable even when the option is not exercised.

Figure 10 reports the distribution of the first hitting time (days to first boundary crossing), conditional on switching. Most switches occur during the middle of the production season, with substantial dispersion around the mean. A non-negligible fraction of hive-years never switch within the annual horizon, reflecting the existence of a sizable inaction region generated by sunk costs and persistent uncertainty. This timing pattern is consistent with migration functioning as a valuable but selectively exercised adaptation strategy.


Figure 10: Distribution of the first hitting time (in days), conditional on switching. Most switches occur mid-season, with wide dispersion reflecting uncertainty and sunk costs.

.

Table 11 reports the main descriptive moments. On average, fewer than one switch occurs per hive-year, consistent with interpreting migration as a one-time and effectively irreversible decision *within the annual horizon* Conditional on switching, the expected payoff at exercise is economically meaningful, while the ex-ante option value is positive and sizable, confirming that flexibility itself has substantial value even when the option is not exercised.

| Statistic | Mean | Std. Dev. |
|---|---|---|
| First hitting time (days, conditional) | 120 | 55 |
| Payoff at exercise (€, conditional) | 21.3 | 14.8 |
| Ex-ante option value (€, unconditional) | 18.1 | 6.4 |

Table 11: Descriptive statistics of switching behavior and option values. First hitting time and payoff at exercise are conditional on switching; the option value is defined for all hive–years.

# 7 Conclusions

This paper analyzes hive mobility as a climate-adaptation decision under uncertainty within a real-options framework. We model the beekeeper's choice between sedentary and migratory management as a reversible switching problem with sunk costs and correlated stochastic returns, embedding mobility in a continuous-time optimal stopping structure. The empirical implementation relies on a high-frequency hive-level panel (2019–2024) combining internal weight dynamics and geolocation data, enabling both the documentation of realized mobility patterns and the calibration of regime-specific diffusion parameters. Four main findings emerge. First, hive-weight dynamics exhibit strong persistence and widespread non-stationarity across both regimes, supporting a stochastic-trend representation and justifying the use of geometric Brownian motion for productivity. Second, realized relocation behavior is strongly directional: movements are predominantly south-to-north and, on average, upslope, consistent with tracking phenological gradients and seeking cooler, later-blooming environments. Third, static regime-by-regime value comparisons reveal a robust migratory premium in expected discounted terms: sedentary values remain tightly concentrated around euro 83-euro 86 per hive-year, whereas migratory values are substantially higher (roughly euro 106-euro 122). This profitability gap remains robust even under conservative drift bands reflecting uncertainty in estimated growth rates. Fourth, once sunk switching costs are incorporated, the optimal policy features a sizable inaction region and selective exercise of the migration option: Monte Carlo policy evaluation shows that switching into migration is infrequent but economically meaningful, whereas reversals within a one-year horizon are rare under average estimated conditions. Earlier boundary crossings are associated with higher discounted payoffs, consistent with the option-value logic of timely adjustment under persistent shocks. Taken together, these findings support a clear interpretation: under climate-driven variability, migration operates as a state-contingent adaptation technology that both enhances expected returns and mitigates localized risk. However, sunk costs generate inertia, delaying adjustment until the expected advantage of relocation is sufficiently persistent. These results have direct implications for climate-adaptation policy. Policies that reduce private switching frictions, such as streamlined permitting, coordinated logistics, and transport infrastructure-can expand the set of productivity states in which mobility is privately optimal. Equally important are information policies that improve anticipatory decision-making, including high-resolution phenology and forage maps, weather-risk alerts, and decision-support tools translating forecasts into expected productivity gains. By lowering effective switching thresholds, such interventions can accelerate efficient adaptation, stabilize hive-level outcomes, and sustain pollination services under increasing climate uncertainty.

Several extensions naturally follow. On the modeling side, the framework can be extended to multiple destination choices, portfolios of hives, endogenous price and cost risk, and Bayesian learning about spatial productivity. On the empirical side, integrating high-frequency weather indicators and floral-resource proxies would help identify the drift and volatility channels more causally and clarify when and where mobility yields the highest insurance value. Despite these avenues for future research, the main message is robust: When climate change generates persistent

and spatially heterogeneous shocks, maintaining the option to relocate becomes a quantitatively significant component of resilient apiculture.

# 8 Appendix

This Appendix collects technical derivations and supplementary empirical evidence supporting the main results of the paper, omitted from the core text for conciseness. Appendix I provides the formal derivation of the Hamilton–Jacobi–Bellman (HJB) equation underlying the switching problem. Starting from the continuous-time Bellman formulation, it applies Itô's lemma to the joint stochastic dynamics of sedentary and migratory productivity and derives the associated variational inequalities, together with the complementarity conditions that characterize the inaction and switching regions. Appendix II presents additional empirical diagnostics on the stochastic properties of hiveweight dynamics. It reports comprehensive stationarity and persistence tests based on Augmented Dickey-Fuller, Hurst exponent, and Variance Ratio methodologies for both mobile and stationary hives over the 2019-2024 period. These results provide independent support for the modeling choice adopted in the paper-namely, treating hive productivity as a highly persistent and non-stationary process.

## 8.1 Appendix - I

This Appendix derives the Hamilton-Jacobi-Bellman equation (3.1), starting from the Bellman formulation (3) and the stochastic dynamics of net returns in (1)–(2).

**Proof.** Let $\pi_s(t)$ and $\pi_m(t)$ denote instantaneous net returns under sedentary and migratory management, respectively. Under (1), their joint dynamics are given by

$$d\pi_k(t) = \mu_k\, \pi_k(t)\, dt + \sigma_k\, \pi_k(t)\, dz_k(t), \qquad k \in \{s, m\},$$

with correlation structure $\mathbb{E}[dz_s(t)\, dz_m(t)] = \rho\, dt$ as in (2).

Let $V_i(\pi_s, \pi_m)$ denote the value function associated with operating under regime $i \in \{s, m\}$. Because the problem is stationary, the value function does not depend explicitly on calendar time. The Bellman equation (3) can be written as

$$V_i(\pi_s, \pi_m) = \max\Big\{\pi_i(t)\, dt + e^{-r\, dt}\, \mathbb{E}[V_i(\pi_s(t+dt), \pi_m(t+dt))]\,,\; V_j(\pi_s, \pi_m) - K_{ij}\Big\}.$$

We focus on the continuation region, where it is optimal to remain in regime $i$. Using the first-order expansion $e^{-r\, dt} = 1 - r\, dt + o(dt)$, subtracting $V_i(\pi_s, \pi_m)$ from both sides, and retaining terms of order $dt$ yields

$$0 = \pi_i(t)\, dt + \mathbb{E}[dV_i] - r\, V_i(\pi_s, \pi_m)\, dt + o(dt).$$

Dividing by $dt$ and letting $dt \to 0$ gives

$$0 = \pi_i(t) + \frac{\mathbb{E}[dV_i]}{dt} - r\, V_i(\pi_s, \pi_m).$$

Applying Itô's lemma to $V_i(\pi_s, \pi_m)$ under the joint diffusion of $(\pi_s, \pi_m)$ implied by (1)–(2) yields

$$dV_i = \sum_{k=s,m} \mu_k \, \pi_k \, \frac{\partial V_i}{\partial \pi_k} \, dt + \frac{1}{2} \sum_{k=s,m} \sigma_k^2 \, \pi_k^2 \, \frac{\partial^2 V_i}{\partial \pi_k^2} \, dt + \rho \, \sigma_s \sigma_m \, \pi_s \pi_m \, \frac{\partial^2 V_i}{\partial \pi_s \, \partial \pi_m} \, dt$$
$$+ \sum_{k=s,m} \sigma_k \, \pi_k \, \frac{\partial V_i}{\partial \pi_k} \, dz_k.$$

Taking expectations and noting that the stochastic (martingale) terms have zero mean, we obtain

$$\frac{\mathbb{E}[dV_i]}{dt} = \sum_{k=s,m} \mu_k \, \pi_k \, \frac{\partial V_i}{\partial \pi_k} + \frac{1}{2} \sum_{k=s,m} \sigma_k^2 \, \pi_k^2 \, \frac{\partial^2 V_i}{\partial \pi_k^2} + \rho \, \sigma_s \sigma_m \, \pi_s \pi_m \, \frac{\partial^2 V_i}{\partial \pi_s \, \partial \pi_m}.$$

Substituting this expression into the continuation condition yields

$$r \, V_i - \pi_i(t) - \sum_{k=s,m} \mu_k \, \pi_k \, \frac{\partial V_i}{\partial \pi_k} - \frac{1}{2} \sum_{k=s,m} \sigma_k^2 \, \pi_k^2 \, \frac{\partial^2 V_i}{\partial \pi_k^2} - \rho \, \sigma_s \sigma_m \, \pi_s \pi_m \, \frac{\partial^2 V_i}{\partial \pi_s \, \partial \pi_m} = 0,$$

which coincides with the infinitesimal generator $\Gamma V_i$ defined in (3.1).

Finally, optimal switching is characterized by the complementarity conditions (4)–(5):

$$\Gamma V_i \geq 0, \qquad V_i(\pi_s, \pi_m) \geq V_j(\pi_s, \pi_m) - K_{ij},$$

with at least one condition binding. These conditions define the inaction region and the switching boundaries $\pi_m = b_{sm}(\pi_s)$ and $\pi_m = b_{ms}(\pi_s)$. ■

## 8.2 Appendix - II

Table 12 summarizes Augmented Dickey–Fuller (ADF) stationarity tests performed on hourly hive-weight series for both mobile and stationary hives over the period 2019–2024. The ADF test is computed under three specifications: ADF_AR (autoregressive with no trend or drift), ADF_ARD (autoregressive with drift), and ADF_TS (autoregressive with trend and drift). For each case, the table reports the total number of hives analyzed, the count and share of non-stationary series (based on a p-value threshold of 0.05), the mean p-value, and the standard deviation of the p-value.

The results reveal a consistent pattern: the majority of hive-weight time series across all years and hive types are identified as non-stationary, with non-stationarity percentages often exceeding 90% under the ADF_AR specification. This pattern is particularly pronounced for mobile hives, which often exhibit even higher non-stationarity rates than stationary hives, suggesting stronger persistence in migratory productivity dynamics.

Allowing for drift (ADF_ARD) and trend (ADF_TS) reduces the fraction of non-stationary series, as expected. However, even under these more flexible specifications, non-stationarity remains prevalent, typically ranging between roughly 66% and 83%. This evidence suggests that hive-weight series follow a non-mean-reverting stochastic trend rather than a stationary process. This is possibly due to the influence of external environmental factors such as temperature, humidity, floral availability, or hive movement patterns.

From a temporal perspective, the stationarity results are remarkably stable across years. For instance, in 2020 and 2023, non-stationarity under ADF_AR reaches 95% and 92.9% respectively, reinforcing the evidence that the stochastic nature of honey weight persists year after year. The p-values also display moderate variability, with standard deviations ranging from approximately 0.31 to 0.42, reflecting heterogeneity in individual hive behaviors.

Overall, the ADF results support the conclusion that hive-weight dynamics are characterized by high persistence and lack of stationarity. This finding has important implications for modeling: it justifies the use of non-stationary diffusion processes rather than strongly mean-reverting specifications. Moreover, the distinction between mobile and stationary hives, and their differing stationarity profiles, underscores the need for tailored modeling strategies depending on the mobility regime.

| Test | Hive Type | Year | Non-Stat. Count | Total | Mean p-value | Std. p-value | NonStat % |
|---|---|---|---|---|---|---|---|
| ADF_AR | mobile | 2019 | 38 | 40 | 0.7352 | 0.2613 | 95.0 % |
| ADF_AR | stationary | 2019 | 58 | 65 | 0.5258 | 0.3150 | 89.2 % |
| ADF_ARD | mobile | 2019 | 28 | 40 | 0.3174 | 0.3328 | 70.0 % |
| ADF_ARD | stationary | 2019 | 51 | 65 | 0.4908 | 0.3689 | 78.5 % |
| ADF_TS | mobile | 2019 | 33 | 40 | 0.4917 | 0.3684 | 82.5 % |
| ADF_TS | stationary | 2019 | 51 | 65 | 0.5326 | 0.4058 | 78.5 % |
| ADF_AR | mobile | 2020 | 294 | 314 | 0.6428 | 0.3243 | 93.6 % |
| ADF_AR | stationary | 2020 | 431 | 449 | 0.6920 | 0.3061 | 96.0 % |
| ADF_ARD | mobile | 2020 | 248 | 314 | 0.4487 | 0.3544 | 79.0 % |
| ADF_ARD | stationary | 2020 | 337 | 449 | 0.4287 | 0.3597 | 75.1 % |
| ADF_TS | mobile | 2020 | 271 | 314 | 0.6041 | 0.3740 | 86.3 % |
| ADF_TS | stationary | 2020 | 365 | 449 | 0.5753 | 0.3877 | 81.3 % |
| ADF_AR | mobile | 2021 | 813 | 851 | 0.6681 | 0.3084 | 95.5 % |
| ADF_AR | stationary | 2021 | 793 | 864 | 0.6040 | 0.3300 | 91.8 % |
| ADF_ARD | mobile | 2021 | 663 | 851 | 0.4306 | 0.3519 | 77.9 % |
| ADF_ARD | stationary | 2021 | 637 | 864 | 0.4113 | 0.3447 | 73.7 % |
| ADF_TS | mobile | 2021 | 683 | 851 | 0.5356 | 0.3844 | 80.3 % |
| ADF_TS | stationary | 2021 | 660 | 864 | 0.5013 | 0.3882 | 76.4 % |
| ADF_AR | mobile | 2022 | 1254 | 1320 | 0.7158 | 0.3084 | 95.0 % |
| ADF_AR | stationary | 2022 | 1236 | 1332 | 0.6345 | 0.3366 | 92.8 % |
| ADF_ARD | mobile | 2022 | 868 | 1320 | 0.4141 | 0.3772 | 65.8 % |
| ADF_ARD | stationary | 2022 | 905 | 1332 | 0.4039 | 0.3672 | 67.9 % |
| ADF_TS | mobile | 2022 | 952 | 1320 | 0.5497 | 0.4258 | 72.1 % |
| ADF_TS | stationary | 2022 | 951 | 1332 | 0.4967 | 0.4143 | 71.4 % |
| ADF_AR | mobile | 2023 | 1526 | 1609 | 0.7146 | 0.3150 | 94.8 % |
| ADF_AR | stationary | 2023 | 1634 | 1794 | 0.6229 | 0.3383 | 91.1 % |
| ADF_ARD | mobile | 2023 | 1251 | 1609 | 0.4899 | 0.3688 | 77.8 % |
| ADF_ARD | stationary | 2023 | 1322 | 1794 | 0.4604 | 0.3730 | 73.7 % |
| ADF_TS | mobile | 2023 | 1333 | 1609 | 0.6071 | 0.3849 | 82.8 % |
| ADF_TS | stationary | 2023 | 1357 | 1794 | 0.5227 | 0.4000 | 75.6 % |
| ADF_AR | mobile | 2024 | 1205 | 1279 | 0.6808 | 0.3195 | 94.2 % |
| ADF_AR | stationary | 2024 | 1397 | 1528 | 0.6311 | 0.3354 | 91.4 % |
| ADF_ARD | mobile | 2024 | 964 | 1279 | 0.4900 | 0.3681 | 75.4 % |
| ADF_ARD | stationary | 2024 | 1236 | 1528 | 0.5176 | 0.3558 | 80.9 % |
| ADF_TS | mobile | 2024 | 1002 | 1279 | 0.5915 | 0.3948 | 78.3 % |
| ADF_TS | stationary | 2024 | 1275 | 1528 | 0.6089 | 0.3717 | 83.4 % |

Table 12: Summary of ADF stationarity test results on honey weight series (2019–2024). NonStat % indicates the share of non-stationary series (p-value $> 0.05$).

Table 13 reports complementary mean-reversion diagnostics based on the Hurst exponent and average p-values from the Variance Ratio (VR) test.

The Hurst exponent remains consistently high throughout the sample (between 0.83 and 0.87), indicating strong tendency toward persistent, non-reverting dynamics. Differences between mobile and stationary hives are modest, although mobile hives tend to display slightly higher persistence in later years.

Mean p-values from the VR test are consistently above conventional 5% significance thresholds. In most cases they lie between 0.08 and 0.15. These values suggest limited evidence of classical mean reversion and are broadly consistent with near-random-walk behavior at high frequency. However, since the average p-values are not extremely low, the strength of mean reversion should be interpreted with caution.

Taken together, these diagnostics indicate that hive-weight dynamics exhibit long-range dependence and persistence, with limited support for strong mean reversion. This persistent structure is consistent with the biological and environmental inertia affecting beekeeping yields. These findings reinforce the modeling choice adopted in the main text: specifications imposing strong mean reversion (e.g., AR(1) processes with $|\phi| < 1$) would be inconsistent with the empirical properties of the data.

| Year | Hive Type | Mean Hurst | Mean VR p-value |
|---|---|---|---|
| 2019 | Mobile | 0.86 | 0.128 |
| 2019 | Stable | 0.83 | 0.129 |
| 2020 | Mobile | 0.85 | 0.084 |
| 2020 | Stable | 0.83 | 0.127 |
| 2021 | Mobile | 0.85 | 0.132 |
| 2021 | Stable | 0.85 | 0.108 |
| 2022 | Mobile | 0.85 | 0.087 |
| 2022 | Stable | 0.85 | 0.135 |
| 2023 | Mobile | 0.86 | 0.094 |
| 2023 | Stable | 0.85 | 0.147 |
| 2024 | Mobile | 0.87 | 0.098 |
| 2024 | Stable | 0.87 | 0.102 |

Table 13: Mean reversion indicators for honey weight (2019–2024). The table reports the average Hurst exponent and average VR test p-values for mobile and stable hives.

**References**

CREA (2025). Honey cost - Sintesi principali risultati economici campagne produttive 2023 - 2024, Fact Sheet. Available at https://www.crea.gov.it/documents/20126/0/HC$_{F}actSheet_{1}.pdf$.

Di Corato, L., & Ginbo, T. (2021). Climate change and coffee farm relocation in Ethiopia: A real-options approach. Climate Change Economics, 12(3), 2150011.

Dixit, A., & Pindyck, R. (1994). *Investment under uncertainty.* Princeton, NJ: Princeton University Press.

EFSA Scientific Committee, More, S., Bampidis, V., Benford, D., Bragard, C., Halldorsson, T., Hernández-Jerez, A., Bennekou, S. H., Koutsoumanis, K., Machera, K., Naegeli, H., Nielsen, S. S., Schlatter, J., Schrenk, D., Silano, V., Turck, D., Younes, M., Arnold, G., Dorne, J.-L., Maggiore, A., Pagani, S., Szentes, C., Terry, S., Tosi, S., Vrbos, D., Zamariola, G., & Rortais, A. (2021). Scientific Opinion on a systems-based approach to the environmental risk assessment of multiple stressors in honey bees. EFSA Journal, 19(5), e06607. https://doi.org/10.2903/j.EFSA2021.6607

Flores, J. M., Gil-Lebrero, S., Gámiz, V., Rodríguez, M. I., Ortiz, M. A., & Quiles, F. J. (2019). Effect of the climate change on honey bee colonies in a temperate Mediterranean zone assessed through remote hive weight monitoring system in conjunction with exhaustive colonies assessment. Science of the Total Environment, 653, 1111–1119. https://doi.org/10.1016/j.scitotenv.2018.11.004

Gajardo-Rojas, M., Muñoz, A. A., Barichivich, J., Klock-Barría, K., Gayo, E. M., Fontúrbel, F. E., Olea, M., Lucas, C. M., & Veas, C. (2022). Declining honey production and beekeeper adaptation to climate change in Chile. Progress in Physical Geography: Earth and Environment, 46(5), 737–756. https://doi.org/10.1177/03091333221093757

Huang, M.-J., Hughes, A. C., Xu, C.-Y., Miao, B.-G., Gao, J., & Peng, Y.-Q. (2022). Mapping the changing distribution of two important pollinating giant honeybees across 21,000 years. Global Ecology and Conservation, 39, e02282. https://doi.org/10.1016/j.gecco.2022.e02282

Le Conte, Y., & Navajas, M. (2008). Climate change: Impact on honey bee populations and diseases. Revue Scientifique et Technique de l'OIE, 27(2), 499–510. https://doi.org/10.20506/rst.27.2.1819

Mahankuda, B., & Tiwari, R. (2024). Impact of climate change on honeybees and crop production. In S. Sheraz Mahdi, R. Singh, & B. Dhekale (Eds.), Adapting to climate change in agriculture - Theories and practices (pp. 171–192). Springer. https://doi.org/10.1007/978-3-031-28142-6_8

Martínez-López, V., Ruiz, C., De la Rúa, P. (2022). Migratory beekeeping and its influence on the prevalence and dispersal of honey bee pathogens. International Journal for Parasitology: Parasites and Wildlife, 18, 184-193. https://doi.org/10.1016/j.ijppaw.2022.05.004

Narita, D., & Quaas, M. (2014). Adaptation to climate change and climate variability: Do it now or wait and see? Climate Change Economics, 5, 1450013.

Neumann, P., & Straub, L. (2023). Beekeeping under climate change. Journal of Apicultural Research, 62(5), 963–968. https://doi.org/10.1080/00218839.2023.2247115

Ostwald, M. M., da Silva, C. R. B., & Seltmann, K. C. (2024). How does climate change impact social bees and bee sociality? Journal of Animal Ecology, 93, 1610–1621. https://doi.org/10.1111/1365-2656.14160

Pilati, L., & Fontana, P. (2020). Sequencing the Movements of Honey Bee Colonies between the Forage Sites with the Microeconomic Model of the Migratory Beekeeper. Beekeeping - New Challenges. IntechOpen. http://dx.doi.org/10.5772/intechopen.80540

Rahimi, E., & Jung, C. (2024). Global Trends in Climate Suitability of Bees: Ups and Downs in a Warming World. Insects, 15(2), 127. https://doi.org/10.3390/insects15020127

Regan, C., Bryan, B., Connor, J., Meyer, W., Ostendorf, B., Zhu, Z., & Bao, C. (2015). Real options analysis for land use management: Methods, application, and implications for policy. Journal of Environmental Management, 161, 144-152.

Remotti, F., Mattalia, G., Porporato, M., et al. (2024). 'The rules of nature are changing; every year is unpredictable': perceptions of climate change by beekeepers of Liguria, NW Italy. Regional Environmental Change, 24, 79. https://doi.org/10.1007/s10113-024-02242-3

Schatzki, T. (2003). Options, uncertainty and sunk costs: An empirical analysis of land use change. Journal of Environmental Economics and Management, 46, 86-105.

Song, F., Zhao, J., & Swinton, S. M. (2011). Switching to perennial energy crops under uncertainty and costly reversibility. American Journal of Agricultural Economics, 93, 768-783.

Swapna, R. K., Saha, S., & Reddy, J. A. (2023). Migratory beekeeping: A boon to both farmer and beekeeper. Insect Environment, 26(1), 65–70.

Tennakoon, S., Apan, A., & Maraseni, T. (2024). Unravelling the impact of climate change on honey bees: An ensemble modelling approach to predict shifts in habitat suitability in Queensland, Australia. Ecology and Evolution, 14(4), e11300. https://doi.org/10.1002/ece3.11300

Van Espen, M., Williams, J. H., Alves, F., Hung, Y., de Graaf, D. C., & Verbeke, W. (2023). Beekeeping in Europe facing climate change: A mixed methods study on perceived impacts and the need to adapt according to stakeholders and beekeepers. Science of the Total Environment, 888, 164255. https://doi.org/10.1016/j.scitotenv.2023.164255

Vercelli, M., Novelli, S., Ferrazzi, P., Lentini, G., & Ferracini, C. (2021). A qualitative analysis of beekeepers' perceptions and farm management adaptations to the impact of climate change on honey bees. Insects, 12(3), 228. https://doi.org/10.3390/insects12030228

Zapata-Hernández, G., Gajardo-Rojas, M., Calderón-Seguel, M., Muñoz, A. A., Yáñez, K. P., Requier, F., Fontúrbel, F. E., Ormeño-Arriagada, P. I., & Arrieta, H. (2024). Advances and knowledge gaps on climate change impacts on honey bees and beekeeping: A systematic review. Global Change Biology, 30(3), e17219. https://doi.org/10.1111/gcb.17219